MARGIT AUN

Dependence of UV radiation on climate factors.
Reconstruction of UV doses in Estonia
for past years

TARTU ÜLIKOOL · SISIS
· UNIVERSITAS TARTUENSIS ·
1632

MARGIT AUN

Dependence of UV radiation on climate factors. Reconstruction of UV doses in Estonia for past years

This study was carried out at the Institute of Physics, University of Tartu, Estonia and Tartu Observatory, Estonia.

Dissertation was accepted for the commencement of the degree of Doctor of Philosophy in environmental technology at the University of Tartu on December 12, 2017 by the Scientific Council on Environmental Technology, University of Tartu.

Supervisors:	PhD Kalju Eerme, Tartu Observatory, Estonia
	Assoc. Prof. Hanno Ohvril, Institute of Physics, University of Tartu, Estonia
Opponents:	PhD Kaisa Lakkala, Finnish Meteorological Institute, Finland
	PhD Enn Kaup, Institute of Geology, Tallinn University of Technology, Estonia
Commencement:	February 17, 2017, University of Tartu, *Physicum*, W. Ostwaldi Str 1

Publication of this thesis is granted by the Institute of Physics, University of Tartu.

European Union
Regional Development Fund   Investing in your future

CONTENTS

ABSTRACT

The thesis is a study of outdoor ultraviolet (UV) radiation as a part of solar radiation – its spectral and temporal variability, doses, as well as dependence on solar elevation, cloudiness, column ozone and aerosols. All conclusions are site-specific, based on measurements carried out at Tõravere, Estonia, since 2004. Special attention is paid to the influence of cloudiness as the main factor modifying solar radiation, including the UV region. Clear sky, totally cloudy and broken cloudiness conditions are intercompared as well as different cloud types. UV doses in overcast days are about 1/3 from the clear weather ones and cloudiness showed wavelength dependence with more radiation passing the clouds at the shorter end of UVA than at the longer end – cloud modification factor in case of overcast sky at 332 nm is 0.38 and at 386 nm 0.36, respectively.

Due to various effects of UV radiation on ecosystems (in particular, humans, animals, plants, microorganisms) and materials, there is a necessity to assess quantitatively UV daily exposures and describe their long-term variations. As spectral measurements of UV radiation are carried out only in short time period (since 2004 at Tõravere) and due to technical reasons, there are gaps in data, models for calculating daily doses for UVA and UVB were developed using freely available ARESLab and libRadtran software. Beside complementing UV database, the models also enabled a retrospective survey on the UV regime in the past, for years 1955–2003. Integrated time series showed a decrease in UVB and UVA yearly doses since the 1970s until the 1980s, mainly due to cloudiness. In both wavelength bands doses have increased since the 1990s, UVB started the increase already in the 1980s. The variability of UV doses is linked with changes in cloudiness observed at Tõravere and changes in column ozone.

The thesis is structured into 4 chapters: 1) introduction, an overview of UV radiation and the objectives of the thesis; 2) data and methods, description of the site, available data from Tartu–Tõravere meteorological station and UV measurements at Tartu Observatory; 3) results, the essential part of the thesis, committed to the results of analysing the influence of clouds and other variables on UV radiation as well as describing the reconstruction using the developed models; 4) conclusions, deems the main results, ongoing and future plans.

I hope that my investigation helps to better understanding of Estonian radiation climate.

LIST OF ORIGINAL PUBLICATIONS

The thesis is based on four publications, referred in the text by Roman numerals. Full texts of the publications are included at the end of the thesis.

I **Aun, M.**, Eerme, K., Ansko, I., Veismann, U., Lätt, S., 2011. Modification of Spectral Ultraviolet Doses by Different Types of Overcast Cloudiness and Atmospheric Aerosol, *Photochemistry and Photobiology*, 87, 461–469.

II Eerme, K., **Aun, M.,** 2012. A Review of the Variations of Optical Remote Sensing Conditions over Estonia in 1958–2011, *International Journal of Remote Sensing Applications*, 2 (3), 12–19.

III Eerme, K., **Aun, M.**, Veismann, U., 2015. Instrumentation and measurement of ground-level ultraviolet irradiance and spectral composition in Estonia, *Solar Radiation Applications*, InTech, 119–139.

IV **Aun M.**, Eerme, K., Aun, M., Ansko, I., 2016. Reconstruction of UVB and UVA radiation at Tõravere, Estonia, for the years 1955–2003, *Proceedings of the Estonian Academy of Sciences*, 65, 1, 50–57.

Author's contribution to the publications
The publications that the dissertation is based on are a result of a collective work with significant input from all the authors. The thesis author's role has been important in all above mentioned publications. Specific work done by the author in each publication (indicated by the Roman numerals) is as follows:

Publication I: The author participated in planning the study, analysed the data, prepared the figures and tables and wrote most of the text.

Publication II: The author processed and prepared some of the data and figures and was involved in the preparation of the text for submitting to the journal.

Publication III: The author processed and prepared some of the data and figures and was involved in the preparation of the text for submitting to the journal.

Publication IV: The author planned the study, leaded the work of building the models and made the calculations. Most of the results were analysed and presented by the author as well as the figures. Most of the text was written by the author.

ACRONYMS

Ac	*Altocumulus*
AERONET	Aerosol Robotic Network
ANN	Artificial neural network
AOD	Aerosol optical depth
BAOD	Broadband aerosol optical depth
BSRN	Baseline Surface Radiation Network
Cb	*Cumulonimbus*
CCD	Charge-coupled device
Ci	*Cirrus*
CMF	Cloud modification factor
Cu	*Cumulus*
DU	Dobson unit
Frnb	*Fractusnimbus*
MARS	Multivariate adaptive regression splines
NASA	National Aeronautics and Space Administration
NIST	National Institute of Standards and Technology, USA
Ns	*Nimbostratus*
OMI	Ozone Monitoring Instrument
Sc	*Stratocumulus*
SD	Standard deviation
SZA	Solar zenith angle
St	*Stratus*
TOA	Top of the atmosphere
TOMS	Total Ozone Mapping Spectrometer
USSR	Union of Soviet Socialist Republics
UV	Ultraviolet
UVA	Ultraviolet radiation in wavelength range 315–400 nm
UVB	Ultraviolet radiation in wavelength range 280–315 nm
UVI	Ultraviolet index
WHO	World Health Organization
WMO	World Meteorological Organization

1. INTRODUCTION

1.1. Overview of UV radiation reaching the ground

Ultraviolet (UV) is an electromagnetic radiation with a wavelength from 10 nm to 400 nm. In outdoors, UV radiation is present in sunlight. It is also produced artificially e.g. by electric arcs and mercury-vapor lamps. Because of absorption by atmospheric ozone, only the longest range of UV, 280–400 nm, is able to penetrate the atmosphere and reach ground level. However, although lacking the energy to ionize atoms, the UV radiation can initiate photochemical re-actions with organic molecules and induce biological phenomena that are greater than simple heating effects. This interval of wavelengths, mainly due to UV biological effects, is split into two smaller spectral ranges: UVB (280–315 nm) and UVA (315–400 nm). Separation between the ranges, 315 nm, has been set by the Second International Congress of Light in Copenhagen in 1932, this boundary definition is accepted by WMO (World Meteorological Organization) and WHO (World Health Organization). Along with 315 nm, a rounded wave-length, 320 nm, is also used as a separation limit (e.g. Parisi and Kimlin, 1997; Rösemann *et al.*, 2011).

The average flux density of solar energy on a surface oriented perpendi-cularly to the solar beam at an average distance between Sun and Earth is called the solar constant, S_0. Actually this is not a constant, a correct term for this quantity is *extraterrestrial solar total irradiance*. Recommended value of S_0 by the WMO is 1367 W/m^2 (calculated by Fröhlich and Brusa, 1981, and Lenoble, 1993, with a standard deviation of 1.6 W/m^2 (0.12%). More recently, the American Society for Testing and Materials (ASTM, 2000) standardized an updated solar spectrum in a considerably wider wavelength's range, 119.5 nm – 1 mm. Integration along this spectrum led to a solar constant, $S_0 = 1366.1$ W/m^2, with an uncertainty at least 0.1% or 1.4 W/m^2. Considering the small un-certainties in both S_0 values (0.1–0.12%) and considerably bigger uncertainties inherent to broadband solar radiation measurements (at least 1%), it is evident that the older WMO solar constant can be still used calculating and modelling atmospheric processes. Even a more rounded value, $S_0 = 1370$ W/m^2, is used in calculations of Earth's overall energy balance (Seinfeld and Pandis, 2006).

UV radiation forms about 7% of total extraterrestrial solar radiation (Foukal, 1990). The radiation is altered when it passes the atmosphere. These changes include fairly stable and well described diurnal and annual changes due to a stable content of a clean and dry atmosphere, but also random variations induced by changes in cloudiness, column ozone and aerosol content.

Astronomical factors influencing UV radiation are: 1) the Earth-Sun distance, 2) the solar zenith angle (SZA) – the angle between the Sun and the zenith. Daily minimum SZA at a certain location depends on geographical latitude.

The most important random factors modulating UV radiation are clouds, ozone and aerosols (Frederick and Steele, 1995; Burrows, 1997; Schwander *et al.*, 2002; Foyo-Moreno *et al.*, 2003; McKenzie *et al.*, 2007). Clouds reflect, absorb and transmit the incoming radiation. Attenuation by clouds depends mainly on sky coverage, but also on the height, structure and optical thickness of clouds. While mostly clouds decrease the radiation level depending on their properties, there have been several studies on cloud enhancing effect (Foyo-Moreno *et al.*, 2003; Staiger *et al.*, 2008; Feister *et al.*, 2015) due to scattering. Calbo *et al.* (2005) gave an extensive comparison of different studies performed about clouds effect on UV radiation.

Ozone is an important absorber of incoming UV radiation, mainly in the UVB part. UVA range is only slightly affected at its shorter wavelengths (Rieder *et al.*, 2010). Aerosols have generally also reducing effect on UV radiation, but the influence is complex as radiative properties of aerosols include both, scattering and absorption characteristics, which are dependent on wavelength (Reuder and Schwander, 1999).

1.2. Importance of UV radiation

UV radiation is measured and studied because of its effects on ecosystems (including humans, animals, plants, microorganisms) and materials, also due to its influence on, for example, atmospheric chemistry, carbon cycle and litter decomposition (Kakani *et al.*, 2003; Outer *et al.*, 2005; Caldwell *et al.*, 2007; Hader *et al.*, 2007; Jackson and Bartek, 2009). Sensitivity to radiation and its impact varies largely among organisms and there are several kinds of molecules and processes, like photosynthesis of plants, which can be affected by all types of UV radiation (Stapleton, 1992; Kakani *et al.*, 2003; Björn, 2007; Kataria *et al.*, 2014). The net effect of UV radiation at the cellular level is a balance of damage and repair of cellular key structures like DNA (De Gruijl and Rebel, 2008; Jackson and Bartek, 2009; McKenzie *et al.*, 2009). Although the focus is mainly on harmful effects, beneficial impacts have also been investigated, for example, vitamin D synthesis (WMO, 2007; Olds, 2010), for which optimal dose is needed as vitamin D photosynthesis takes place in skin at sub-erythemogenic UV doses, while larger exposures destroy vitamin D and increase DNA damage (Orlova *et al.*, 2013).

The nature and magnitude of the UV effect is dependent on the wavelength, because shorter electromagnetic waves carry higher energy and are therefore more powerful (McKenzie *et al.*, 2007). Different reactions can occur on a certain energy threshold level and therefore it is important to know, beside the total amount of UV radiation energy, its spectral composition. The effects of UV radiation and those of other environmental factors at different levels are not well known yet. Recently many personal UV radiation exposure studies have been carried out (e.g. Bodekær *et al.*, 2015; Baczynska *et al.*, 2016).

For informing the public about the level of UV radiation reaching the Earth's surface and its potential harmful effects on human health the UV index (UVI) is being used. It is a measure of erythemal UV radiation on a horizontal surface and describes the ability of UV radiation to induce erythema (reddening and damaging of the skin). Erythemal action spectrum has been set by the International Commission of Illumination (CIE) in 1987 and again in 1999 (SO 17166:1999(E)/CIE S 007-1998). UVI is defined by a formula:

$$I_{\mathrm{UV}} = k_{\mathrm{er}} \cdot \int_{250\,\mathrm{nm}}^{400\,\mathrm{nm}} E_\lambda \cdot s_{\mathrm{er}}(\lambda) d\lambda \,,$$

where E_λ is the solar spectral irradiance expressed in $\mathrm{W/(m^2 nm)}$ at wavelength λ and $d\lambda$ is the wavelength interval, $s_{\mathrm{er}}(\lambda)$ is the erythema reference action spectrum and k_{er} is a constant equal to 40 $\mathrm{m^2/W}$ (WHO, 2002). The UVI is defined by the CIE with CIE S 013/E:2003 International Standard Global Solar UV Index. The value goes from zero upwards – the larger the number, the more harmful radiation.

In most applications of the UV radiation, data on quantification of the received spectral doses and understanding of the mechanisms of influence on different objects and processes are needed. Spectral measurements allow the data to be applied to any biological or photochemical process with known action spectrum, describing the rate of physiological activity in different wavelengths. Weather conditions prescribing the availability and spectral composition of ground-reaching UV irradiance in key phenological phases of ecosystem manifest significant year-to-year changes. These changes are reflected in ecosystem's health and productivity. For sustainable agriculture and environmental management, both the changes in composition of received irradiance and in ecosystem responses need to be investigated on a quantitative term.

1.3. Measurements and modelling of UV radiation

From a climatological point of view, measurements of UV radiation, at various stations around the world, have been carried out in a relatively short period, during only the last few decades. Regular measurements started with broadband filter instruments in the late 1970s and spectral measurements were added in the early 1990s (WMO, 1995).

Due to fairly short UV radiation time series and therefore lack of detailed spectral information, several techniques for modelling and reconstructing past UV doses have been developed. These methods generally bind together different input climate factors related to UV radiation, and allow, using models (i.e. empirical formulae), calculation of UV radiation doses.

The input characteristics for modelling include the main actinometric radiation fluxes (global, direct, and diffuse), sunshine duration, description of cloudiness, column aerosols and ozone, etc. Some methods use calculated or previously measured clear-sky UV values as an extra input (Mayer *et al.*, 1997; Kaurola *et al.*, 2000; Lindfors *et al.*, 2007). For more complex, sophisticated modelling, methods like Multivariate Adaptive Regression Splines (MARS) technique, introduced by Friedman (1991), and artificial neural networks (ANN) have been used (Krzyscin *et al.*, 2004; Feister *et al.*, 2008; Medhaug *et al.*, 2009; Junk *et al.*, 2012). Most methods are used for daily doses calculations as sorter temporal interval input data are often unavailable.

1.4. Objectives of the thesis

There are 5 general objectives of the thesis:
1. Quantifying the diurnal and seasonal changes in UV spectral composition in Tõravere.
2. Quantifying the different effect of cloudiness and aerosol on different wavelength bands for Tõravere site.
3. Study the variations in cloudiness over Tõravere on seasonal and yearly scales.
4. Developing method and models for UVB and UVA daily dose calculations.
5. Showing the large variability in yearly doses of UV radiation in Estonia and linking them to changes in total solar radiation (because of cloudiness) and ozone.

The thesis includes four published publications.

Publication I is focused on analysing the measured UV irradiation data and finding the influence of clouds and aerosol on spectral UV radiation composition and quantity.

Publication II analyses the cloudiness data and describes the changes over Estonia during 1958–2011 to better understand the importance of clouds on UV radiation reaching the ground.

Publication III is concentrated on description of UV datasets for Tõravere – what type of UV-related data are available, what kind of instruments have been used. Also the description of spectral composition of UV radiation is given in various conditions in spring and summer.

In the final, publication IV, using earlier work, models have been developed for calculation of UVB and UVA daily doses. These models enabled compilation of UV time series for 1955–2003, i.e for years prior to spectral measurements at Tõravere. All together we have now, for 1955–2015, time series of daily doses for UVB and UVA. Analysis of these 61-years long time series showed that UV yearly doses manifest large year to year fluctuations, but have also longer term changes – generally larger UV levels until the 1970s, after that a decrease in UV levels until the 1990s and a steady increase since then.

2. DATA AND METHODS

2.1. Site description

The research done in publications I–IV is based on measurements at Tartu Observatory and Tartu-Tõravere Meteorological station (58°16'N, 26°28'E, 70 m a.s.l.). The territory is surrounded by natural and managed ecosystems including arable fields, grasslands and coniferous forests and therefore can be considered as a rural site in terms of air pollution and atmospheric aerosols. In cooperation with the meteorological station a lot of supporting data were available for analysing changes in UV radiation.

2.2. Meteorological data from Tartu-Tõravere meteorological station

The first attempts to quantitative measurements of solar radiation were made in Tartu in 1904 with the Hvolson actinometer. The first high quality observations of broadband direct solar radiation in Estonia, during 1931–1940, were carried out at the Meteorological Observatory of the University of Tartu. The observatory was located in the building of the governmental archives (Liivi Str. 4). The measurements were performed from an open window of the building, using an Ångström pyrheliometer Nr. 197. Unfortunately this highly valuable device was destroyed during the war in 1944. In the early 1950s new efforts initiated by Acad. Juhan Ross began. From 1950 to 1965 the station was a part of the present research institute Tartu Observatory and since 1965 it was operated by the Estonian Meteorological and Hydrological Institute (Kallis *et al.*, 2005; Ohvril *et al.*, 2009). In 1999 the station was included to the system of Baseline Surface Radiation Network (BSRN) stations which currently includes 67 stations around the world. Until 1996 the Yanishevski AT-50 actinometers and Savinov-Yanishevski M-115 pyranometers were used and then complemented/ replaced by the Eppley Labor. Inc. pyrheliometers and Kipp & Zonen pyrano-meters. The accuracy of the ventilated Kipp & Zonen pyranometers is about ±2% and that of the pyrheliometers ±1%. In the past, inter-calibration of sensors was regularly performed in Voeikov Main Geophysical Observatory (St. Petersburg, Russia), whereas it is now done in the World Radiation Center (Davos, Switzerland) (Eerme *et al.*, 2015). In 2013 Tõravere meteorological station was reorganized to a part of the Estonian Environmental Agency as a State Meteorological Service.

General climatic features of the broadband solar radiation in Estonia are presented in the Handbook of Estonian Solar Radiation Climate (Russak and Kallis, 2003). Major results on interannual and intraseasonal variations of broadband solar radiation in Estonia are presented as a chapter in the book *Solar Radiation* (Eerme, 2012) and partly by Eerme *et al.* (2010).

Regular meteorological observations have been performed in Tartu by the EMHI since July 1957, including the hourly visual cloud detection where sky coverage in tenths in three basic levels and dominating cloud type is marked. Also snow-cover measurements are performed regularly.

Column aerosol information, before year 2002 at Tõravere, is available indirectly using two quantities: 1) pyrheliometer-measured direct solar beam, 2) precipitable water, evaluated from surface water vapor pressure. These quantities allow, either direct calculation of spectral aerosol optical depth AOD550 or calculation of broadband aerosol optical depth (BAOD) with a following transition to AOD500 (Kannel *et al*., 2012, 2014). In 2002, Tartu Observatory joined NASA Aerosol Robotic Network (AERONET) and a sun photometer, CIMEL CE-318, measuring AOD at different wavelengths, precipitable water vapour (*W*) and aerosol microphysical properties, started to operate. The CIMEL sun photometers are circulated between stations and recalibrated by NASA once a year. The calibration and system description is available on the NASA AERONET page: http://aeronet.gsfc.nasa.gov/new_web/system_descriptions.html (last accessed November 15, 2016) and done by Holben *et al*. (1998). It provides AOD data in the spectral range of 340–1020 nm in case of no coverage of the Sun by clouds. From November to February data are sparse due to low sun and heavy cloudiness. Higher aerosol loadings commonly tend to appear in spring and in July–August, but there are differences between years. The lowest AOD values genrally occur in autumn (September–November). Aerosol loadings at Tõravere are strongly influenced by wind direction, as there are no major stationary anthropogenic pollution sources nearby (Russak, 1996). A steady increase in AOD550 occurred in Estonia from 1951 to 1982 due to the growth in industry, agriculture and transport as well as volcanically active years. After that, except the Pinatubo-years, 1991–1993), a rapid decrease occurred due to measures taken to protect the environment (Russak *et al*., 2007; Ohvril *et al*., 2009).

Direct sun column ozone measurements have been regularly carried out at Tõravere between 1994–1999 using an especially suited laboratory spectrometer SDL-1 supplied with a mirror system and applying the Dobson retrieval algorithm (Eerme *et al*., 1998, 2002a). Since 2003, direct sun column ozone measurements have been performed using a MICROTOPS-II instrument. In the present studies total ozone values used are mostly from TOMS (Total Ozone Mapping Spectrometer) and OMI (Ozone Monitoring Instrument) datasets. The average ratio of MICROTOPS-II/OMI values has been 1.002 with SD ± 2.3%, which is about ±8 Dobson Units (DU) (Aun *et al*., 2011). Atmospheric column ozone at Tõravere manifests an annual cycle with the maximum around 390 DU in March–April and a minimum of around 270–280 DU in October-November (Eerme *et al*., 2002a). From the first half of May until the middle of September the column ozone decreases quite linearly and the variations around this linear decrease are mostly moderate, within ± 20 DU. Larger variations have been recorded from February until the middle of May, and also in October-November. Within that period, prolonged episodes reaching a week or even more in length

have been recorded when column ozone has been even more than 50 DU lower than its normal seasonal level.

2.3. UV measurements at Tõravere

Solar UV radiation measurements started at Tartu-Tõravere meteorological station with erythemally-weighted broadband sensors UV-SET in January 1998 (Eerme *et al.*, 2000, 2002b; Veismann *et al.*, 2000). A Kipp & Zonen narrow-band filter instrument CUVB1, with an effective wavelength 306±0.2 nm and bandwidth 2±0.5 nm, operates at Tartu-Tõravere meteorological station since 2002 (Eerme *et al.*, 2006). A Kipp & Zonen broadband UVA sensor as well as a YES broadband UVB sensor were installed at the site in 2005.

Spectral UV measurements at Tartu Observatory, conducted by the work-group of remote sensing of the atmosphere, started in 2004 with Avantes Inc. minispectrometer AvaSpec-256 (Figure 1). The technical description of the system is presented in Publication I, Ansko *et al.* (2008) and briefly in the following part of the thesis. This instrument included 4 m long quartz fiber with 100 µm diameter connected to thermostat. The spectrometer was kept at constant temperature of 7 °C. UFS-5 glass optical filter was installed between the diffuser and fiber to reduce the stray light inside the spectrometer. The optical interface was covered by a shutter after every measurement to detect noise level. Control of the sensitivity for the uniform recording of spectra was realized through the change of integrating time within the interval 1 to 60 s.

Figure 1. AvaSpec-256 in thermal box (left) and optical head with shutter mechanism at the roof of Tartu Observatory (right).

A maximum value of the signal, approximately 16,000 arbitrary units, was recorded in each spectrum. Radiometric response of the system was established using the National Institute of Standards and Technology (NIST, USA) traceable quartz FEL lamps. The most restricting factors were the stray light level in the instrument and a relatively narrow dynamic range of the CCD array sensor. Because the array sensitivity decreased with time, the system needed frequent recalibration and the expected exploitation time of the instrument was only 5–6 years. The intrinsic stray-light problems limit the use of array spectrometers in the UVB region. A program for compensatory calculation of the stray light influence was applied in several investigations (Brown *et al*., 2003; Zong *et al*., 2006; Ansko *et al*., 2008). The slit-scattering function of the spectrometer was measured directly using a 450 W xenon arc lamp source and a monochromator. The stray-light level of the AvaSpec-256 spectrometer was rather high (0.1–1%), but the slit-scattering function was symmetrical and without noticeable artefacts. Because of this, a simplified semi-empirical stray-light removal algorithm was used to correct the spectra (Ylianttila *et al*., 2005). The algorithm was tested against the deconvolution technique (Kostkowski, 1997), and proved to be sufficient. In 2009 the measurements with AvaSpec-256 were stopped due to the significant drop of array sensitivity.

Figure 2. Bentham DMc150F-U inside station (left) and measuring head on the roof of Tõravere meteorological station (right).

Another spectrometric system based on the Bentham Instruments Ltd. DMc150F-U double monochromator (Figure 2) was installed in spring 2009. For the Bentham double monochromator, a calibrator CL 6 belonging to the set

of spectrometer auxiliary instruments is regularly used for checking the instruments' sensitivity and the calibrator itself is regularly compared against a certified FEL lamp.

With both spectrometers UV upper hemispheric spectra, in the range of 280–400 nm, have been recorded regularly in every 15 min from sunrise to sunset with a spectral resolution of about 1 nm. No usable signal can be recorded at the shorter end of the spectrum due to very low or no radiation. The starting wavelength of considerable data depends on SZA. Around summer solstice about 75 measurements are available during a day and about 25 around winter solstice. All spectra are retained in a database.

3. RESULTS

3.1. Main features of annual and daily fluctuations of UV radiation in clear sky conditions

As described earlier UV irradiance and its spectral composition are strongly dependent on SZA and the availability of direct sunshine. SZA manifests regular daily and annual changes, during a day it starts from maximum value at sunrise, reaches the lowest value at noon in True Solar Time and goes back to maximum at sunset. The annual cycle of noon SZA includes the largest value at winter solstice and the lowest at summer solstice. At Tõravere the limits for noon SZA values are 81.7° and 34.8°, respectively.

The following description of changes in cloudless conditions is mainly from publication III.

In the days around summer solstice, the threshold of the Bentham double monochromator's sensitivity allows detection of UV at about 295 nm at noon with clear solar disc. In early mornings and late evenings, the detection drops to approximately 310 nm (Figure 3). In cloudy weather, the irradiance levels are generally lower and the threshold of detection can be several nanometers larger than in clear conditions. This is due to lower spectral irradiance levels of shorter wavelengths and as the UV radiation travels through the atmosphere, this part of radiation is more attenuated than the longer wavelengths part. So the larger the SZA the smaller portion of short wavelength radiation reaches the ground. For that, the accuracy of spectral irradiance measurements is significantly lower when the Sun is near the horizon, SZA > 80°, when solar radiation is weak and the influence of column ozone and aerosols on its spectral composition is less clear.
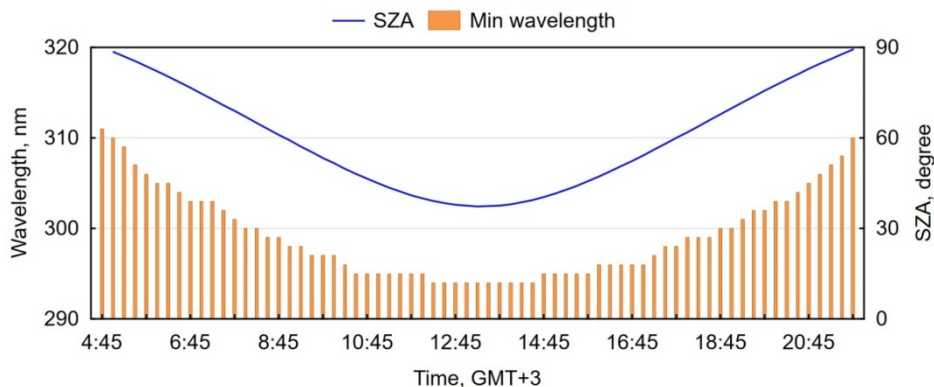

Figure 3. Diurnal cycles of SZA and shortwave threshold for detection of UVB irradiance in midsummer cloudless conditions, 18 July 2010.

While the width of recorded UVA wavelengths is 85 nm (315–400 nm) in all cases, the width of recorded UVB varies significantly. By definition it is 35 nm (280–315 nm), but the observed range can be even as short as 5 nm (310–315 nm) and generally doesn't exceed 20 (295–315 nm). Because the wavelength range of UVB is varying, the ratio of the received irradiance energy or power also varies across a wide range. Increase in SZA enhances the difference between UVA and UVB, the last decreases faster. As a result, a "UVB-day" is considerably shorter than a "UVA-day". In Figure 4, there is an example of diurnal change of spectral irradiances at four selected wavelengths during an almost clear day, July 12, 2010. Column ozone was 299 DU and the average AOD340 = 0.428, i.e. relatively large (multiannual median value for July at Tõravere, AOD340 ≈ 0.27). Squared Sun-Earth distance at July 12, 2010 was 1.034 and noon SZA = 36.29°.
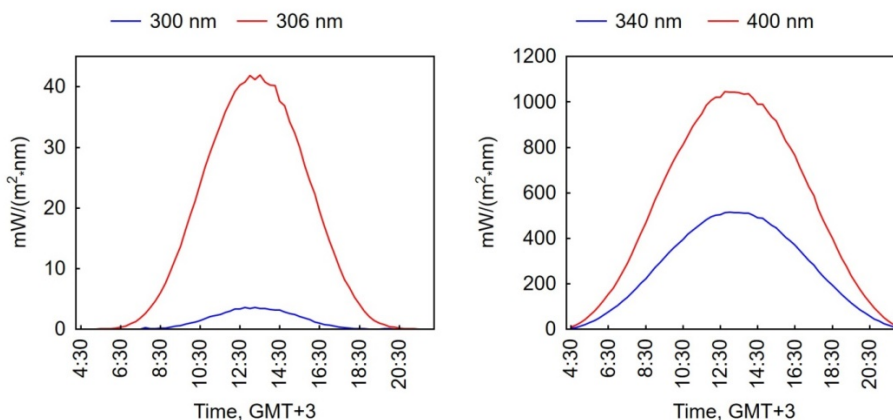

Figure 4. Diurnal cycles of spectral irradiance at selected wavelengths (300, 306, 340 and 400 nm) from UVB (left) and UVA (right) wavelength band on July 12, 2010 in local zonal time (GMT+3).

The attenuation factor at different wavelengths was calculated to detect its spectral features. The atmospheric attenuation essentially increases towards shorter part of UV radiation, e.g. the attenuation factor at 400 nm was 1.6 but at 300 nm, 112.0 (Table 1). Apparently, increase in attenuation towards shorter wavelengths is due to absorption because increase in Rayleigh scattering gives, (400 nm/300 nm)^4 = 3.16 only.

Table 1. Calculation of atmospheric noon attenuation factors for clear sky UV radiation at selected four wavelengths (300, 306, 340 and 400 nm), July 12, 2010, Tõravere

Wavelength, nm	Noon spectral irradiance, mW/(m^2 nm)			Atmospheric attenuation factor
	Ground level, noon	Spectral solar constant	Solar constant, corrected to Sun-Earth distance	
300	3.6	416.6	403.1	112.0
306	41.2	542.2	524.6	12.7
340	513.8	1133	1096.2	2.1
400	1042.9	1727	1670.9	1.6

The ratio of UVA/UVB shows also strong diurnal cycle. Just after sunrise and before sunset the UVB irradiance is strongly suppressed and the value of the UVA/UVB ratio often reaches 500 to 600 at SZA ≈ 87°. For larger SZA the UVB measurements are not reliable at Tõravere. The ratio starts to decrease with the decreasing SZA and the smallest UVA/UVB values are met around the daily smallest SZA. Around summer solstice the range of diurnal changes in the UVA/UVB ratio can reach 15 times. With the decrease of SZA to 70° the ratio UVA/UVB drops to about 100 and after reaching SZA ≈ 50° to about 50. An example of diurnal change in UVA/UVB ratio is in Figure 5.
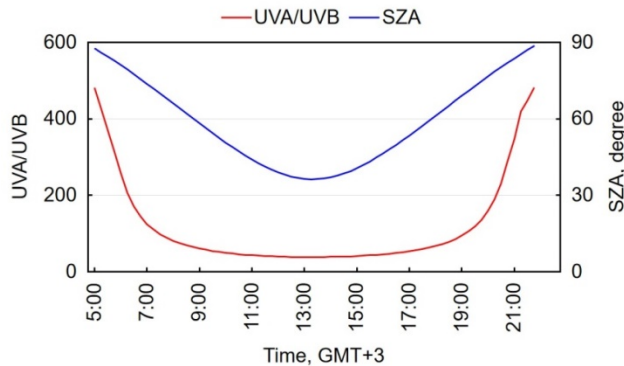

Figure 5. Diurnal cycle of UVA/UVB irradiance ratio in almost clear summer day, 12 July 2010, in local zonal time.

In the Northern European summer conditions most of the UV radiation is received during six hours around noon. The contribution of those 6 hours is relevant indicator from May to August, when irradiance levels are the highest and when the outdoor activities of the population take place frequently in

sunshine. For example in July at wavelengths around 300 nm the contribution from these six hours is 85 to 90% of the daily total, and decreases with increasing wavelength due to decrease of ozone absorption. Around the wavelength 330 nm the noon six hours contribution reaches 60% and remains at an almost constant level for longer wavelengths (Figure 6).
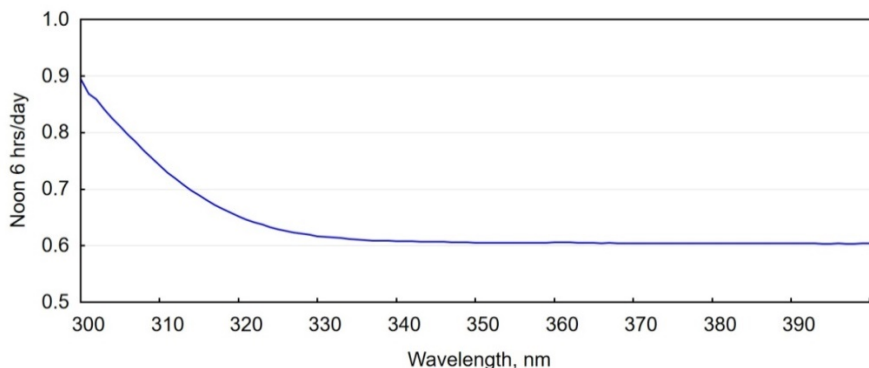

Figure 6. Contribution of UV dose from 6 noon hours to daily total dose at Tõravere, 12 July 2010. For wavelengths > 330 the contribution is almost constant.

3.2. Influence of clouds on UV radiation

Cloudiness, because of its dimensions, extent and variability, plays multiple critical roles in the atmosphere. For an outside of planet observer, clouds represent bright objects in the UV and visible part of the solar spectrum increasing planetary albedo and contributing to the cooling of the planet, thus mitigating the greenhouse effect.

From the variety of parameters used to characterize cloudiness the most fundamental is "cloud amount" (or "degree of cloud cover"), a fraction given in oktas (eighths), tenths or percents. The data are available from Tõravere meteorological station where cloudiness is marked on 3 levels with main cloud types.

3.2.1. Changes in spectral composition of UV radiation

At the study site (Tõravere) the sky is not clear for the majority of the days, therefore the effect of clouds on UV radiation must be considered. The influence of clouds on UV spectral composition is discussed in publications I and III.

Clouds can significantly reduce the ground level irradiance, but also enhance it through scattering. To show the large variability of diurnal spectral irradiances some examples of diurnal cycle of irradiances at single wavelengths are presented in Figure 7 for different type of cloudiness varying both with cloud type and amount.
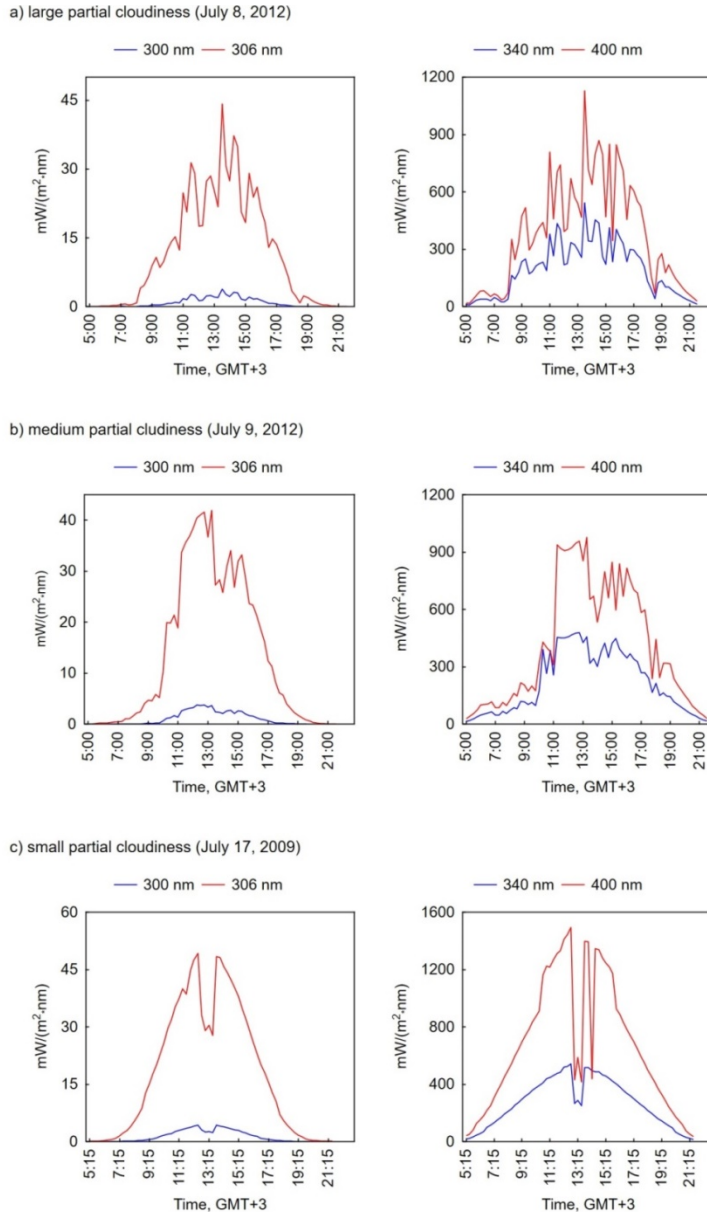
Figure 7. Spectral irradiances for different partial cloudiness amounts at selected UVB (left; 300, 306 nm) and UVA (right; 340, 400 nm) wavelengths: a) large amount of partial cloudiness (8 July, 2012) b) medium amount of partial cloudiness (9 July, 2012) and c) small amount of partial cloudiness (17 July, 2009). Distinguishing of cloudiness amounts has been done on the basis of broadband direct radiation amount compared to clear sky conditions (large 0.7–0.9: medium 0.4–0.6; small 0.1–0.3).

For different partial cloudiness conditions the daily broadband direct irradiance, in regard to clear sky conditions, was calculated and is presented in Table 2 with the description of cloudiness. All of these 3 cases can be considered as typical "good weather" cloud conditions in the summer months. As shown in the presence of clouds the variation of irradiances is large, affecting strongly also the daily dose, especially when the clouds are covering the sun during noon hours.

Table 2. Description of different days with partial cloudiness. Cloudiness classification has been done based on measured broadband direct radiation amount compared to clear sky conditions (large 0.7–0.9; medium 0.4–0.6; small 0.1–0.3)

Partial cloudiness	Cloud types	Date	Global broadband (measured direct)/(direct clear)
Large	*Ci, Cb, Cu, Ac*	July 8, 2012	0.29
Medium	*Ci, Cb, Cu, Ac*	July 9, 2012	0.49
Small	*Ci, Cu*	July 17, 2009	0.82

To characterize the cloud effect, cloud modification factor (CMF) was used, defined as,

$$\text{CMF} = \frac{\text{UV}_{\text{cloudy}}}{\text{UV}_{\text{clear}}},$$

where UV can represent both, irradiance or dose. When solar disc is shaded by clouds the irradiance is reduced and CMF < 1. In the case of clear Sun, but clouds nearby it, the irradiance can be temporarily enhanced and the CMF > 1. Examples of both situations are shown in Figure 8. Enhanced situation is from July 7, 2011 with varying cloudiness (*Cu*, *Cb* and *Ac*), the clear measurement is taken from July 11, 2010 with similar SZA. Attenuated situation is from July 1, 2010.

The CMF shows an impressive increase, up to a factor of 1.6 at 392 nm, during the enhanced situation. In an attenuation case, decrease of CMF toward longer wavelengths in UVA wavelength band is shown, illustrating the wavelength dependency of cloud effect on UV radiation. The behavior of CMF around 300 nm is influenced by ozone. The daily total effect mainly depends on the cloudiness characteristics during the noon hours, when most of the energy is received.
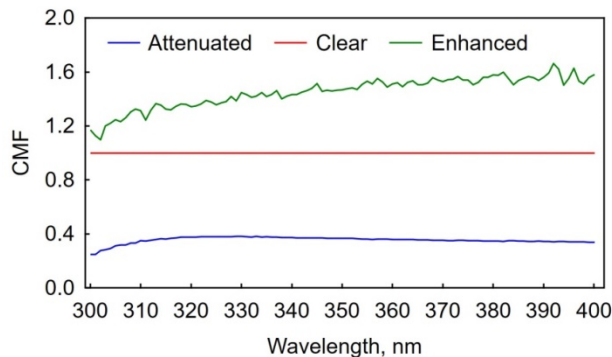
Figure 8. Example of enhancement and attenuation of UV spectral irradiance by clouds at SZA around 36°. In attenuated situation (blue line) the CMF, measured irradiance (July 1, 2010) divided with clear conditions (July 11, 2010), is below 1, in enhanced situation (green line) the CMF, measured irradiance (July 7, 2011) divided with clear conditions (July 11, 2010) is above 1.

3.2.2. Overcast conditions

The investigation of overcast cloudiness on UV radiation was carried out using the data of AvaSpec-256 collected in 2004–2008. Clear and overcast days were selected from the dataset, based on the daily ratio of measured broadband direct solar irradiance (0.305–2.8 μm, μm for Kipp & Zonen pyranometers; Russak and Kallis, 2003) to its normal conditions clear day value. For clear days the threshold was set to 0.95 and for overcast days 0.05. Days with strong precipitation and days with noon SZA above 80°, Decembr 1 – January 11, were excluded. Daily doses of UVB, UVA, as well as doses spectral densities at 8 selected wavelengths (306, 315, 322, 332, 346, 353, 371 and 386 nm) were calculated. The specific wavelengths were selected from "stable" spectral regions.

However, in the first stage of investigation only days with noon SZA less than 45° were included, covering the period between April 25 and August 17. In total 27 overcast and 14 clear days met established conditions. The numbers are small, since neither of the circumstances is typical for warm season at Tõravere.

For both spectral ranges, UVB and UVA, basic statistics were calculated (Table 3). Somewhat surprising were the high UV radiation levels during overcast days. On the average the daily doses of overcast days were about 1/3 of clear day values. UVB daily doses were slightly more reduced due to clouds, compared those of UVA. It can partly be explained by moderately different ozone levels and aerosol loadings. The median value of total ozone was 342 DU for overcast and 339 DU for clear weather. Also the mean SZA was around 1.5 degrees larger for overcast days, amplifying the influence of different column ozone. The ratio UVA/UVB is higher in cloudy condition by 13%.

Table 3. Basic statistics of UVB and UVA daily doses for clear and overcast days with noon SZA from 35 to 45° (between April 25 and August 17, 2004–2008)

	CLEAR SKY					OVERCAST SKY				
	Mean	Median	Min.	Max.	Std. dev.	Mean	Median	Min.	Max.	Std. dev.
UVB, kJ/m^2	28.91	28.77	22.12	36.74	3.71	9.67	9.45	4.71	17.58	2.98
UVA, MJ/m^2	1.46	1.46	1.23	1.62	0.01	0.55	0.54	0.33	0.88	0.13
UVA/UVB	51.07	50.66	44.10	62.33	4.67	58.45	56.10	48.82	76.81	8.06

Results in Table 3 suggest that around noon UVB and UVA doses received during three overcast hours are approximately equal to one hour doses of clear sky.

For the same selection of data daily doses at selected wavelengths were analysed. In general, as expected, doses increased as wavelength increases, both, in clear and overcast days, except for 386 nm compared to 371 nm possibly due to absorption by Fraunhofer Fe I line.

For all the selected wavelengths the CMF for daily doses were calculated (Figure 9). The CMF is smallest at 306 nm where beside cloud influence ozone plays important role as a reducer of UV radiation. In the UVA range, above 332 nm, where ozone has almost no influence CMF decreases towards longer wavelengths showing wavelength dependency of cloud attenuation perhaps partly due to weaker Rayleigh scattering in longer wavelengths (Kylling *et al*., 1997).
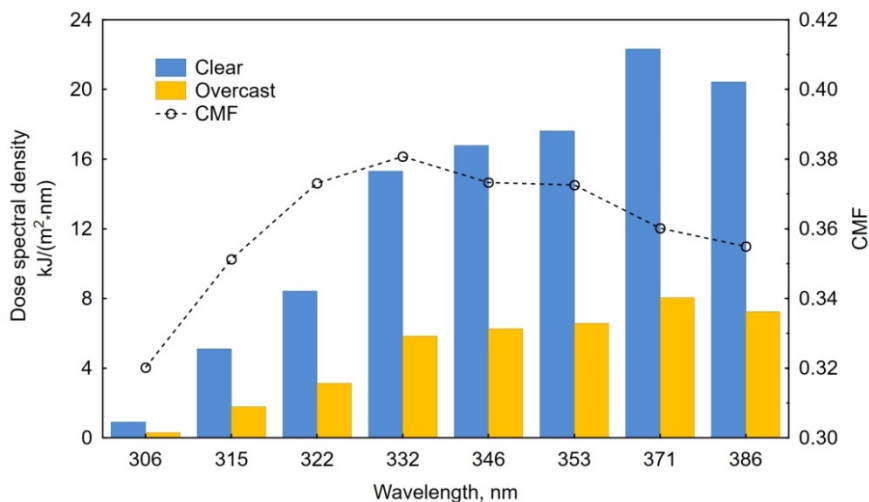

Figure 9. Mean spectral densities of daily doses for clear and overcast days with noon SZA below 45°. Course of cloud modification factor, CMF=UV$_{cloudy}$/UV$_{clear}$.

As the next step impact of SZA on spectral composition was studied. Both, overcast and clear days from the initial selection (354 days) were divided into 3 groups based on noon SZA intervals (35–50°, 50–65° and 65–80°). Median columns ozone values were checked for all groups and additional selection was carried out in order to uniform the median ozone. For all groups mean daily spectral doses were calculated (Figure 10). In groups with the lower sun, noon SZA over 50° spring and fall days were also separated because of seasonal trends in column ozone. Spectral doses in UVB tend to be higher in fall compared to spring due to higher spring ozone values.
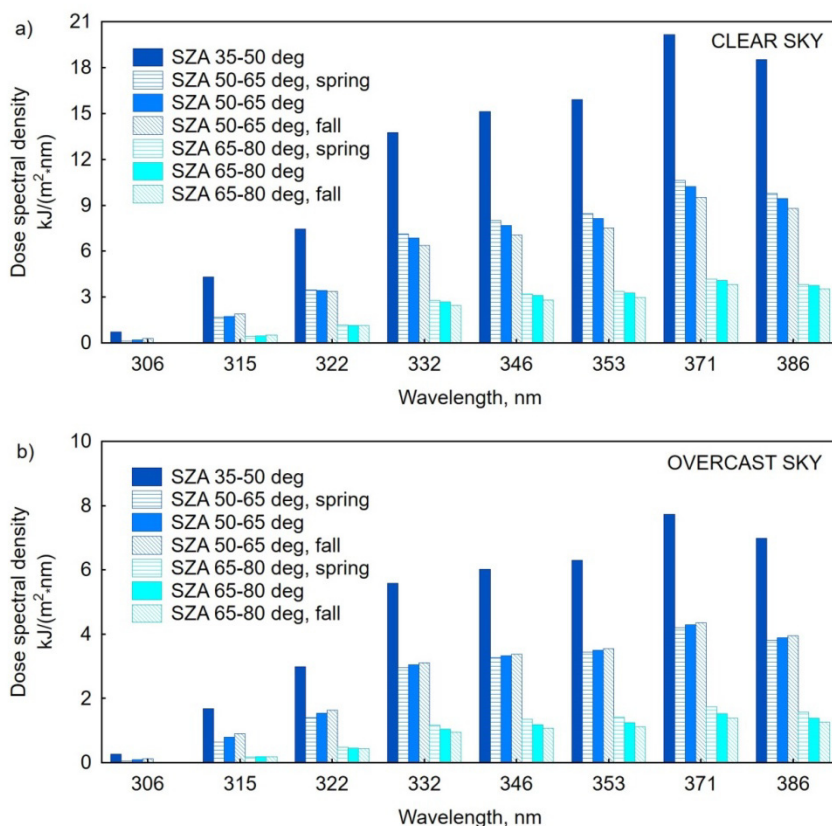

Figure 10. Mean spectral densities of daily doses for clear (a) and overcast (b) days in 3 separated noon SZA groups. In groups with noon SZA 50°–65° and 65°–80° spring and fall are presented separately also.

Figure 11 demonstrates the difference between the smallest (35°–50°) and largest (65°–80°) noon SZA groups, spring and fall combined. The largest reduction of irradiance and dose due to the increase of mean noon SZA appeared in UVB region (306 and 315 nm). At 306 nm the mean daily dose of

the largest SZA group was around 95% smaller than in the smallest noon SZA group. At large SZA, the optical path is longer and attenuation by ozone becomes more evident. In the UVA spectral range (322, 332, 346, 353, 371, 386 nm) the reduction due to higher SZA was stable, around 80% in clear condition and 83–84% in overcast conditions. It can be concluded, that the decrease of CMF toward longer wavelengths in the UVA range does not depend significantly on SZA, but in UVB region the dependence is strong.
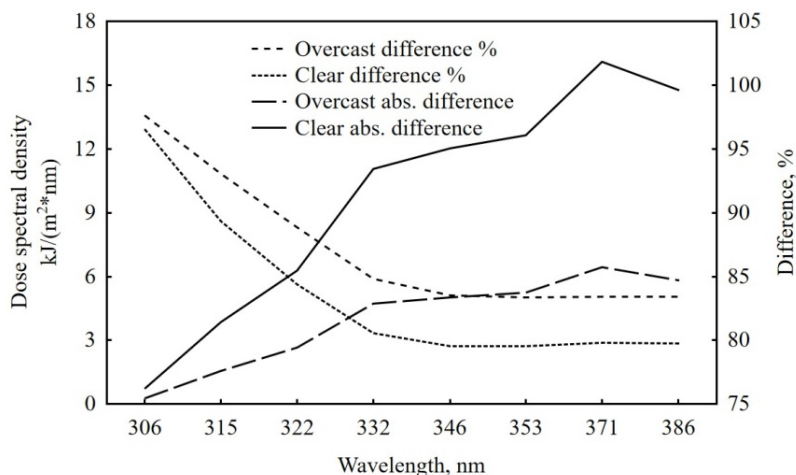

Figure 11. Difference of doses spectral densities between the lowest (35–50°) and highest (65–80°) noon SZA group.

3.2.3. Different cloud types

Because clouds optical properties are highly variable comparison of different cloudiness types and also some specific case studies of different type of cloudiness was carried out on the data of AvaSpec-256 from 2004–2008. Common cloud types of *St*, *Ns*, *As* and *Ac* were chosen to see differences of CMF between cloud type. In publication I for each cloudy condition similar clear situation (SZA ± 1° and total ozone ± 30 DU) was chosen. Later the same analyse was carried out using calculated clear sky values with libRadtran software for better overlap of SZA and column ozone. New calculations gave similar results. The CMF mean values for different cloud types are presented in Table 4. For *Ns* 743, *St* 663, *As* 24 and for *Ac* 109 measurements were included. The CMF mean values were, as expected, higher for medium level clouds (0.66 and 0.61 in UVB) compared to low level clouds (0.35 and 0.45 in UVB), but the range of CMFs was wide and there were similar values found in different cloud types so in case of single measurement no separation can be made based on CMF.

Table 4. CMF mean values and ranges mean $\pm$ SD for different cloud types

Cloud type	UVB		UVA	
	Mean	Mean $\pm$ SD	Mean	Mean $\pm$ SD
Ns	0.35	0.14 – 0.55	0.31	0.15 – 0.47
St	0.45	0.26 – 0.65	0.38	0.22 – 0.53
As	0.61	0.49 – 0.73	0.51	0.41 – 0.60
Ac	0.66	0.43 – 0.90	0.55	0.38 – 0.71

For each cloud type cloudy periods from single days were also selected. Single case studies also demonstrate the large variability in CMF. For UVB irradiances, the changes through selected episodes are presented in Figure 12. No clear difference can be made between cloud types.
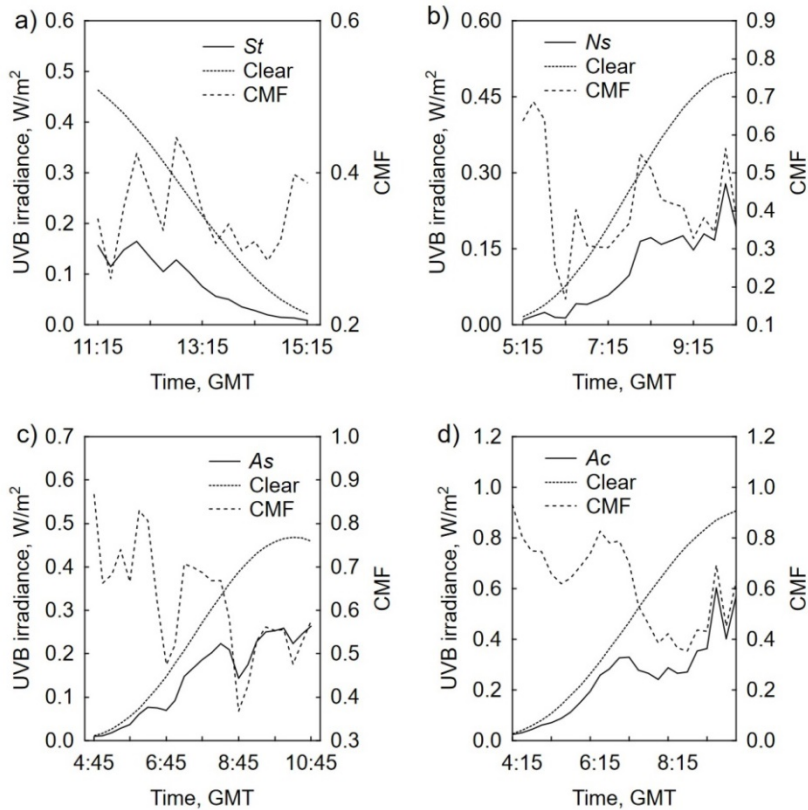

Figure 12. Comparison of different cloud types and clear day UVB irradiances and CMF for a) *St;* b) *Ns; c) As*; d) *Ac* cloudiness.

3.3. Variability of cloudiness at Tõravere

Cloudiness modulates solar radiation and restricts optical remote sensing from satellites. In frames of this research, an extensive analyse on changes in cloudiness over Tõravere was carried out. It is presented in publication II, including interannual and seasonal variations in the amounts of summarized, lower plus medium level, and separately, upper level clouds as seen in spaces free from lower and medium level clouds. Years from 1958–2011 were considered, based on hourly visual detection of clouds at the Tartu-Tõravere meteorological station.

According to hourly visual estimations (half past each hour), two different datasets on "relative" cloud amounts are compiled. Note that the "absolute" cloud amount, i.e. the probability of the presence of a cloud at the observer's zenith (Leonoble, 1985), is usually not included into routine meteorological measurements. The first dataset is rather usual consisting of: 1) relative total cloud amount (in tenths, on a scale of 0–10), as a compound of clouds at all three levels, 2) relative amount of lower clouds, 3) types of clouds. This dataset was previously used by Russak (1990) who calculated monthly mean amounts for low and total clouds, respectively. She found that during 23 years, 1964−1986, the mean annual relative cloud amount of low clouds increased by 11%. Note that according to the traditional synop codes used in the former USSR, the term "low clouds" was used for the following cloud types: *Cu*, *Cb*, *St*, *Sc*, *Ns*, *Frnb*. Although for total cloudiness a reliable trend was not found, behavior of low clouds was in line with decrease in the Bouguer coefficient of column transparency, apparently due to volcanically active years, there were 12 great volcanic eruptions during 1963−1982 (Ohvril *et al*., 2009). The last research was enhanced to monthly means of total cloudiness and low clouds for the 41-year period, 1955−1995, including visual observations at 16 meteorological stations in Estonia (Keevallik and Russak, 2001). All data were downloaded from the archives of the former Estonian Meteorological and Hydrological Institute (now Estonian Environment Agency). The authors found that on the basis of annual averages, no definite conclusions can be drawn on the trends in the amounts of low clouds in Estonia. Concerning seasonal variability, the authors established similar courses for both, total cloudiness and for low clouds: a maximum amount in November-December and a minimum in June. The most impressive feature was the increase in the amount of low clouds in March at all 16 stations. The authors ascribed this phenomenon to changes in the European large scale atmospheric motions − increase of westerlies with more cyclones from the Atlantic to the east, which leads to a shift of spring to an earlier period.

Besides standard observations on total cloudiness and low clouds at Tõravere, clouds were detected, since July 1957, separately at each of three basic altitude levels. These unique observations were analysed for 1958−2011 in a paper by Eerme and Aun (2012) due to clouds influence on UV radiation and remote sensing. It is interesting to note that somewhat a similar problem of

evaluation of possibilities to perform optical observations through the atmosphere became actual in the astrophysics since the 1950s. Worsening of observing conditions in old observatories placed inside or close to towns caused allocation domes of new telescopes at sites with less cloudiness and urbanization. A special term, "astroclimate", was introduced in order to characterize atmospheric conditions favorable for astrophysics. Estimation of the availability of relevant conditions for observing the Earth from space may be denominated as the "remote sensing climate".

As the clouds on two lower levels are almost nontransparent, their total amount (lower clouds + intermediate clouds) was considered together in our analysis, separately from the upper level (Ci) clouds.

In addition to traditional monthly averages, in order to achieve a better climatological temporal resolution, single observations on cloudiness were averaged over 10 days. In each month, the third decade was actually 8–11 days long, depending on the month's length. Each year consists of 36 decades, there were 1944 decades during 54 years, 1958–2011.

3.3.1. Low and medium level clouds

A matrix of sky coverage by sums of low and medium level clouds consists of 54 rows (years) and 36 columns (decades). Visualization of the matrix of 1944 elements in a carpet-type Figure 13 allows showcasing significant interannual variations. In cold winters with frequent domination of high pressure the monthly averages are much lower than in warm cyclonic winters. In February smaller cloud amounts appear more frequently before 1985. In July higher cloud coverage is present from the 1970s to the 1990s, before and after the cloud amounts are smaller. The probability density distributions for a single year is negatively skewed and generally the median is 0.1–0.4 tenths larger than mean. The monthly cloudiness is highest in November and December, exceeding 8 tenths. Generally January and February are also heavily cloudy. Overcast conditions are met more frequently from October to February. Since then, average cloudiness decreases to around 5 tenths in the last decade of April. Approximately the same average coverage persists until the middle of June when it increases by 0.5 tenths and remains on the same level until the middle of August.
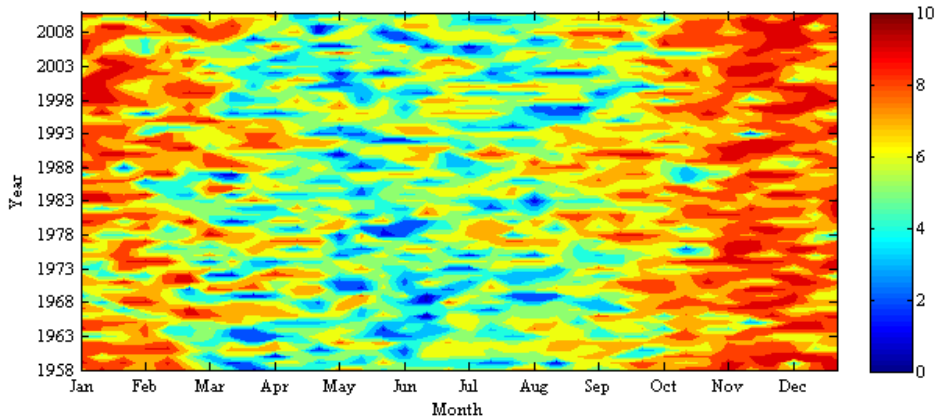
Figure 13. Amounts of low + medium level clouds in tenths during 54 years, 1958–2011, averaged over ten days (36 periods per year).

3.3.2. High level clouds

Besides of low + medium level clouds, there remains a restriction of remote sensing by Ci clouds. Amount of Ci clouds, for a ground based observer, can be assessed from spaces in the sky, which are clear from low and medium level clouds. This type of study has been made earlier, for years 1958–2003 (Eerme, 2004). Further, in the work by Eerme and Aun (2012) the data from years 2004–2011 were added and a new survey was made.

Days with a relative coverage of the sky with spaces, free from low and medium level clouds, above 1 tenth, were selected for further Ci cloud detection. Only the period from March to September was selected for analysing the amount of Ci clouds. The remaining months were excluded due to commonly appearing heavy cloudiness and therefore lack of days with suitable cloud conditions. The monthly variations of average and max/min number of included days in 1958–2011 are presented in Figure 14. The figure shows, how the number of days, with at least 1 tenth of sky free from lower level clouds increases from March to July and declines after that.
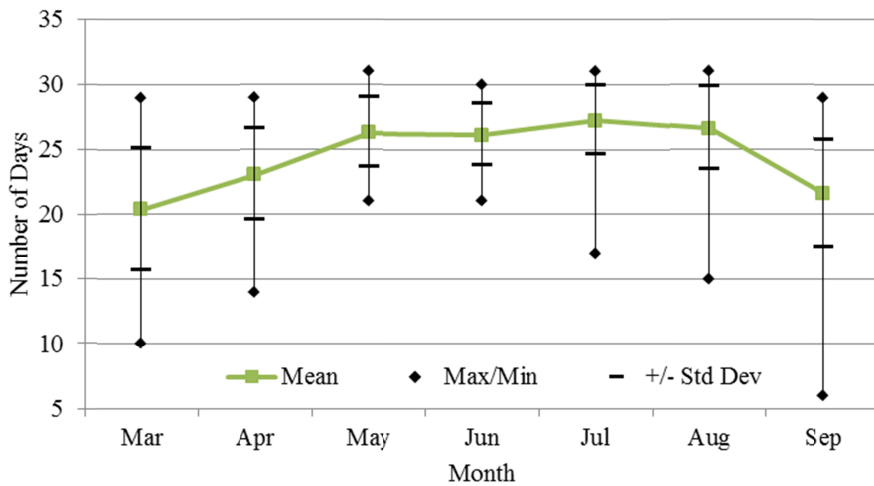
Figure 14. Monthly averages of days with daily average spaces free from low and medium level clouds above 1 tenth from March to September. Monthly averages, StDev limits, and max/min number of days from 1958–2011 are presented.

Figure 15 represents long term (1958–2011) changes in annual total number of days, from March to September, with daily average spaces, in low + medium level clouds, above 1 tenth. Noticeable is: 1) a general large year-to-year variability, and 2) a period with lower number of considered days at the beginning of the 1990s. The last observation can be partly related to the increase of concentration of cloud condensation nuclei formed by falling from the stratosphere sulphate aerosol after the Mt. Pinatubo eruption in June of 1991.
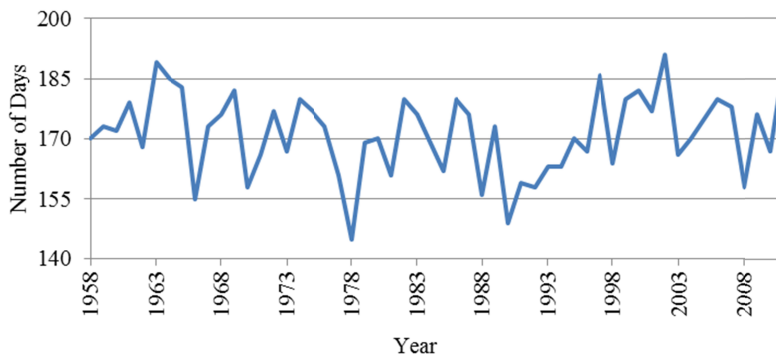

Figure 15. Annual total number of days in March to September with daily average spaces free from low and medium level clouds above 1 tenth from 1958–2011.

The relative coverage of the spaces free from low + medium level clouds from March to September (months suitable for high level clouds observations) is highest in April, declines until minimum average value in July and increase again after that (Figure 16).
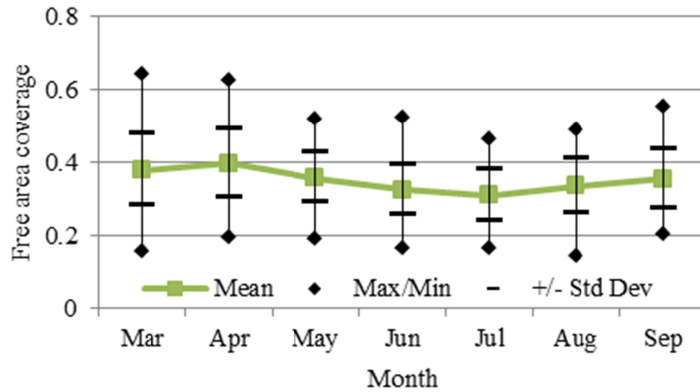

Figure 16. Average relative coverage of spaces, free from low + medium level clouds, with high level clouds from March to September (1958–2011).

Averaged over the period from March to September values of coverage by cirrus clouds varies within range 0.26 to 0.45, with the mean value 0.35. Time evolution of average relative coverage of spaces, free from low + medium level clouds in warmer months (March – September) showed larger values during the beginning of the 1990s and lower values from 2002 to 2007. Longer compact period with positive deviation in years 1992–1996 is probably related to the increased aerosol content after eruption of Mt Pinatubo in 1991.

3.3.3. Cloud-free noon hours

An assessment of variability and changes of days presenting cloud-free conditions within ±2 hours from the noon was carried out as most of the energy is collected during that time and for remote sensing smaller SZA and cloud free conditions are preferred. The annual average number of suitable days, days with no clouds ±2 hours from the noon, was 26.7 and maximum was 50. Two most minimal annual values, 12 and 13, were recorded in recent decade, in years 2004, 2008 and 2009.

In Table 5, are the statistics of number of days with cloud-free noon hours from the period 1958–2011 in monthly and seasonal scale, respectively for winter (JFM), spring (AMJ), summer (JAS), autumn (OND).

Table 5. Monthly and seasonal averages and maxima of days suitable, no clouds ±2 hours from the noon, for optical remote sensing, in 1958–2011. Also the number of years out of 54 and percent of years with no suitable days. The same on seasonal scale

Month	Average	Maximum	Years with no suitable days	
			Number	*Per cent*
January	2.07	6	11	20.4
February	2.41	9	17	31.4
March	3.83	14	6	11.1
April	2.78	7	9	16.7
May	3.09	10	9	16.7
June	2.52	8	13	24.1
July	2.61	13	15	27.8
August	1.65	11	18	33.3
September	1.52	5	19	35.2
October	1.61	9	20	37
November	1	8	28	51.9
December	1.54	6	14	25.9
Winter	8.31	20	0	0
Spring	8.39	17	0	0
Summer	5.78	20	3	5.5
Autumn	4.15	13	2	3.7

March is the most favorable month for remote sensing at Tõravere, followed by May and April. The monthly average number of such suitable days was the smallest, only one, in November. In winter the numbers suitable for remote sensing increase in the presence of cold high pressure conditions.

In conclusion it can be stated that cloudy conditions are prevailing in Estonia and therefore clouds play a major role in modulating UV radiation, also the conditions for remote sensing in Estonia are moderate. The monthly number of days with clear noon hours tends to be relatively low and manifest strong interannual variations. For each month a number of years with no suitable conditions were found. The percent was highest for November (51.9%) and lowest for March (11.1%).

Despite the fact that the daily average amount of low and medium level clouds are smaller in spring and summer compared to the rest of the year, the remote sensing conditions are not the best for summer due to convective clouds during noon hours.

Since the late 1980s the conditions for optical remote sensing at the study site have rather worsened in winter and spring as well as on annual level as shown in Figure 17.
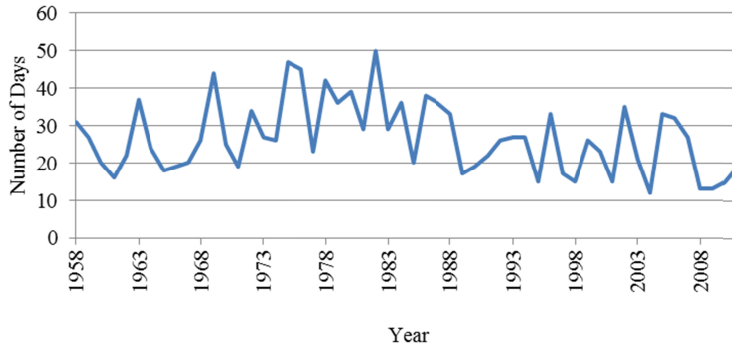

Figure 17. Annual numbers of days with cloud free noon hours (± 2 hours from noon) and therefore suitable for optical remote sensing from 1958–2011.

The changes in cloudiness are partly in line with the general changes in atmospheric transparency, presented in Figure 18, reflecting the column aerosol load. The end of the 1970s and the beginning of the 1980s manifested several major volcanic eruptions that substantially increased the amount of atmospheric aerosols and declined column transparency. In context of clouds, aerosols are important for cloud formation.
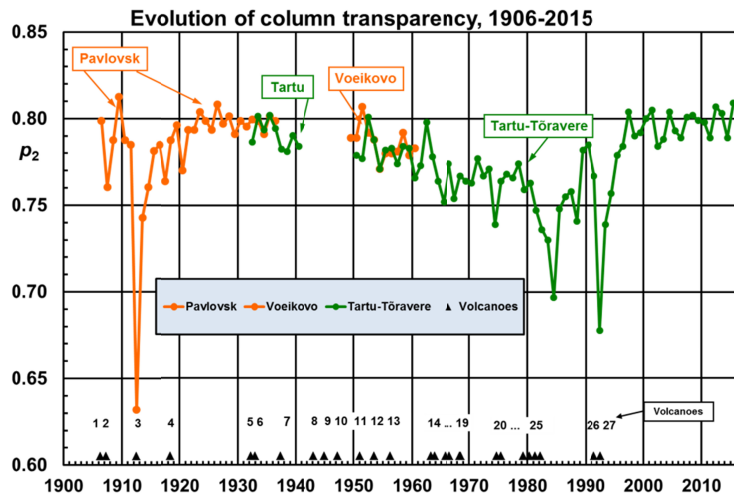

Figure 18. Evolution of atmospheric column integral transparency coefficient, p_2 (the index means that optical mass $m = 2$, solar elevation $\approx 30°$), during 1906–2015 (courtesy by H. Ohvril).

3.4. Aerosol effects on UV radiation

Aerosol effects on UV radiation become important in the cases of large AOD levels, when attenuation of UV radiation is enhanced. For estimating aerosol influence, some case studies were performed. Four almost clear days from 2006 were chosen: 27th April, 1st, 4th and 5th May. From the selection, two days were marked cloud free, one day had 1.4 tenths (daily average) of *Ci* clouds near the horizon and 1 day 0.2 tenths of *Ac* clouds after 7 p.m. During these days AOD340 was stably large, varying between 0.979 and 1.299. The background value of AOD340 at Tõravere is about 0.2 and in 2002–2012 the AERONET system recorded AOD340 values above the threefold and twofold median at Tartu-Tõravere meteorological station in about 6% and 17%, respectively, out of 1500 days of the AERONET measurement data from period 2002–2012.

Days with large AOD were compared against single clear day (May 1, 2007), with similar noon SZA, total ozone (384 DU, for high AOD episode between 379 and 391 DU) and low AOD340 (0.16). UVB and UVA daily doses of selected clear day with low AOD340 and mean daily doses for the days with high AOD340 are presented in Table 6.

Table 6. Mean daily doses for UVB and UVA for 4 days with high AOD level and for 1 clear day with similar SZA and normal AOD level

	Normal AOD (1 day)	High AOD, Mean (4 days)	UV (high AOD)/ UV (normal AOD)
UVB kJ/m²	14.42	10.74	0.74
UVA MJ/m²	0.99	0.83	0.84
UVA/UVB	68.68	77.61	

For the days with high AOD levels the mean daily dose of UVB was 74% of clear day dose and 84% for UVA. The ratio of the daily dose at single wave-lengths measured on days with high AOD values and on clear day showed wavelength dependency. The ratio at 306 nm was 0.71 and at 386 nm 0.86 (Figure 19). Compared to clouds effect the influence at UVA region is in opposite direction – longer wavelengths are less affected.
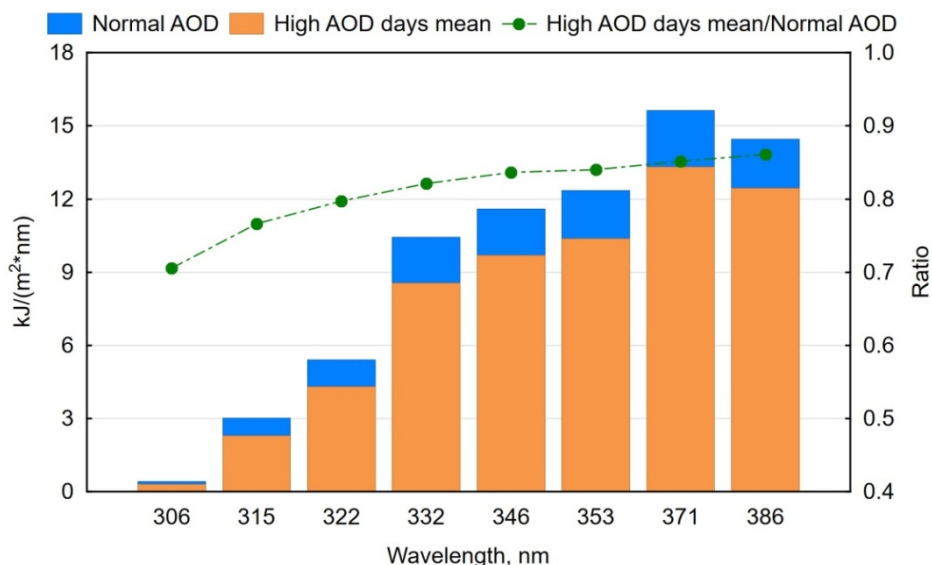
Figure 19. Comparison of mean daily spectral UV doses for a group of days manifesting smoke induced large AOD340 against a clear day (with almost equal noon SZA, similar column ozone 384 DU and AOD340=0.16).

The wavelength dependency of aerosol effect on UV radiation can be explained by aerosol-size distribution that is characterized by the fine mode fraction, e.g., how much the submicronic particles contribute to the AOD. Smoke often contributes more than 90% of small particles' influence in AOD, reducing radiation more strongly at shorter wavelengths (Krzyscin *et al*., 2004; Niemi *et al*., 2005; Barnaba *et al*., 2011; Witte *et al*., 2011). In the chosen days the high AOD values were most likely caused by fires. Much larger values than usual of AOD were recorded in many different sites during the period April 25 to May 6, 2006. This long episode is related to biomass burning in Eastern Europe (Arola *et al*., 2007; Lund Myhre *et al*., 2007; Stohl *et al*., 2007; Amiridis *et al*., 2010). The total burned area in the Baltic countries, Russia, and Ukraine reached 2 million hectares and more than 300 fires per day were detected in the region above 40 degrees North and between 20 degrees and 60 degrees East. Most of the fires were located in Russia, Byelorussia and Ukraine. A great majority of fires were detected over cropland whereas the number of those detected over wooded grasslands, woodlands and grasslands remained modest.

3.5. Reconstruction of past UV doses for Tõravere

3.5.1. Modelling method

Spectral UV measurements started at Tõravere in 2004. However, there are strong reasons to continue elaboration of alternative, model based evaluations for the UV radiation, for instant spectral irradiances as well as for doses. A climatological example of this kind of necessity is a retrospective (for Tõravere, years before 2004) or prospective (for future years) retrieval of the UV radiation. Another need is a quick UV radiation estimation in order to fill empty gaps in a recorded time series which may happen due to instrumentation problems. And sometimes, during a later inspection the recorded data may seem too low (underestimated) for a certain period. As usual in solar irradiance observations, a doubt arises about an undesirable object (insect, spider's thread, trash, dust, snow, etc) dwelling on the instrument's dome. When at the same time solar broadband irradiances were also recorded, an alternative UV radiation estimation, through model approaches, exists and gives a possibility to evaluate performed UV radiation recordings.

A variety of UV radiation reconstruction methods have been developed over the last two decades (Haberreiter *et al*., 2005; Lindfors and Vuilleumier, 2005; Eerme *et al*., 2006; Outer *et al*., 2010; Bilbao *et al*., 2011). Most methods use observations and measurements of other climate- and UV-related quantities, for example broadband solar radiation measurements, cloud observations, column ozone values etc. Also modelling of clear-sky UV irradiance values have been used (Mayer *et al*., 1997; Kaurola *et al*., 2000; Lindfors *et al*., 2007). More complex models have been built using artificial neural networks (Feister *et al*., 2008; Medhaug *et al*., 2009; Junk *et al*., 2012) and Multivariate Adaptive Regression Splines (MARS) (Krzyscin *et al*., 2004). Majority of the models are made for erythemal UV calculations.

For reconstruction of past UV daily doses at Tõravere the period 1955–2003 was chosen because of availability of classic actinometric solar radiation measurements and beginning of UV radiation measurements in 2004. Freely available ARESLab and libRadtran software were selected for constructing the models. ARESLab is a Matlab/Octave toolbox for building piecewise-linear and piecewise-cubic regression models using MARS technique (Jekabsons, 2011). The MARS modelling is a form of regression analysis introduced by Jerome H. Friedman (1991). In a simplest form it describes nonlinearities as a sum of linear functions. In general, MARS builds models in the form of weighted sum of basis functions $B_i(x)$:

$$\hat{y} = \sum_{i=1}^{k} c_i B_i(x),$$

where each c_i is a constant coefficient, the "hat" on the y indicates that it is a predicted value to an input x. MARS builds a model in two phases. In the first, forward phase, all database fields are tested by adding basis functions to get the largest reduction in the training error. At the end of the first phase, a large model that overfits the data is built, which means the model works well with data used for building the model, but does not perform well with new data. In the second, backward deletion phase, the model is simplified by deleting least important basis functions based on generalized cross validation value, which is calculated using the mean squared error and model parameters (Krzyścin, 2003; Jekabsons, 2011).

The other used software package, libRadtran, is a set of tools for radiative transfer calculations in the Earth's atmosphere. Its main instrument is the *uvspec* program which calculates the radiation field in the Earth's atmosphere under variety of atmospheric conditions (Mayer and Kylling, 2005).

In our work, the first step was calculations of clear-sky UVB and UVA irradiances and SZAs using libRadtran version 1.6-beta and its *uvspec* model. The *uvspec* program includes a number of different radiative transfer equation solvers. We have chosen the DISORT2, which enables calculation of downward direct and diffuse UV irradiance. Among other settings, from proposed standard atmospheres 'mid-latitude winter' and 'mid-latitude summer' were selected. The summer season lasted from 21 March to 22 September. Correction of extraterrestrial irradiance for the Sun–Earth distance was made by an included time function.

Total (column) ozone daily values, mainly from satellites, are available since 1979. In the cases of single missing daily data, monthly averages of the respective year were applied. Prior to 1979 the monthly averages of column ozone for 1979–1989 were selected as the best estimation. Because the average ozone values started to decrease from the 1980s, the used values can be by few percentage points lower than actual values. This estimation is made based on the WMO (1991) report that showed a decrease in ozone column of 4.7% per decade for May to August 1978–1991 in St. Petersburg (60° N), a close location to Tõravere site. Lower ozone values can cause some overestimation of the modelled UVB levels but as the main factors (SZA and cloudiness) influencing UV radiation have a much stronger influence and variation, this difference is not decisive, especially considering that day-to-day variations of ozone can also be larger. Due to technical problems with TOMS data, there are large data gaps in column ozone values during 1993–1996. For filling the data gaps in the case of less than 15 available daily values for a month, monthly averages from 1990–1999 were used.

The albedo for the measurement site was chosen 0.4 for snow and 0.03 for snow-free conditions as it has been used by other authors (Schwander *et al*., 1999; Rieder *et al*., 2008) although albedo for fresh snow can reach much higher values (even above 0.9), the average value due to snow age, purity and fragmentation at the measurement site is lower.

Due to lack of aerosol data at the study site (before 2002), aerosol was partly described by standard built-in options of libRadtran: rural type of aerosol was selected and two seasons were used: spring–summer (March–August) and autumn–winter (September–February). The Ångstrom wavelength exponent (α) was retrieved for each calendar month as average for 2002–2010 from the AERONET archives. For December, due to lack of data, January average value was used assuming similar conditions of both months. In the period 2004–2009 only one year, 2006, had systematically larger than usual AOD values during a longer period, from 25 April to 6 May, caused by extensive landscape fires in Eastern Europe (Stohl *et al*., 2007). In other years the spread of fires was rather moderate, and relatively large AOD values appeared only as short events. Global dimming and brightening i.e. decrease and increase in shortwave solar radiation and also in UVA separately that are due to changes in the atmospheric aerosol load, described by for example Zerefos *et al*. (2009) and also by many other authors (e.g. Stanhill, 2005; Wild *et al*., 2005; Cutforth and Judiesch, 2007; Kambezidis *et al*., 2012) are included in the present work only through the measured global solar radiation as an input to ARESlab. In Estonia more and less cloudy periods alternate solar radiation strongly. In cloudy conditions it is difficult to assess the role of aerosols.

The UV irradiance calculations with libRadtran were made after every 15 min for both wavelength ranges for every day from 1955 to 2003 and the daily doses were integrated. Also daily noon SZAs were derived from libRadtran calculations.

The models were built using ARESLab which uses training data cases with x_i as input data and y as an a priori known output. Altogether 440 days of measurements from 2004–2006 were used for training. Rest of the days from chosen period were excluded due to gaps in AvaSpec-256 measurements (more than 2 consecutive measurements missing, missing measurements at the beginning or at the end of the day) or for too large noon SZA (>80 degrees, from December 1 to January 11). Daily doses of UVB and UVA radiation were calculated from measured irradiances, standardized, and later used as a known output. Standardized value was found as:

$$z = \frac{X - \mu}{\sigma},$$

where z is the standardized value, X is the measured value, μ the mean and σ the standard deviation. Summarizing the input parameters: global solar radiation daily dose, daily column ozone, noon SZA and clear-sky UVB and UVA daily doses. Also snow cover and cloudiness were tested as input data, but these had no or only insignificant impact to the model's performance. It might be due to their impact on measured global solar radiation that is already included. Input values were normalized in the range 0 to 1.

3.5.2. Testing of the models

The testing of the models to evaluate their performance was carried out with the data collected in 2007 (200 days). Both, UVB and UVA, models showed good results manifesting linear correlation coefficients and coefficients of determinations of measured and calculated daily doses above 0.98 (Figure 20).
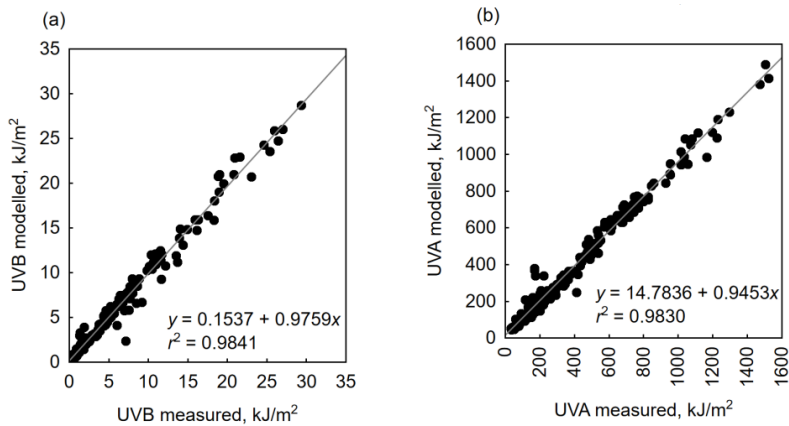

Figure 20. Scatterplot of measured and modelled UV daily doses in 2007 for (a) UVB and (b) UVA. 200 days are included.

The daily doses of measured and modelled UVB and UVA radiation can be seen in Figure 21 and publication IV. No notable systematic difference to either side was detected. The sum of the modelled daily doses of the days used for testing for UVA was only about 2% smaller than the sum of the measured doses. The modelled daily UV doses had lower peak values in the summer period. For UVB the difference in peak values was smaller. In general, the modelled values were less precise in colder months (NDJF), partly due to the presence of snow, which makes the radiation field more complex. The inaccuracy of the model increases also with SZA. The higher relative difference in winter is also due to much lower absolute vales of measured irradiance, making even a small difference in doses significant in relative values. However, doses from that period play a minor role in the yearly total.
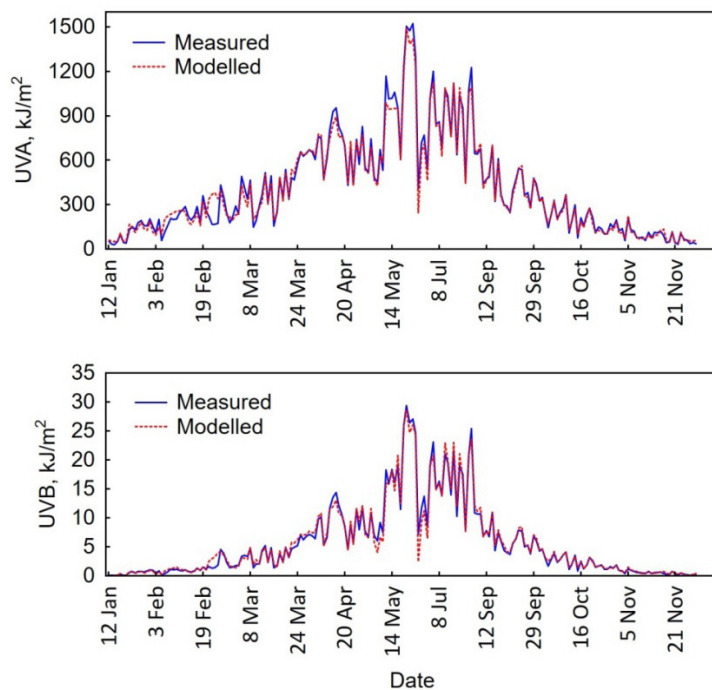
Figure 21. Comparison of 200 measured and modelled UVB (a) and UVA (b) daily doses in 2007.

The models were also tested against data received from Bentham DMc150F-U measurements. The period from 1 April to 30 September 2012 was chosen to give a preliminary evaluation for the suitability of the models to fill data gaps from different instruments. For the chosen time frame of 183 days, 101 had measurements. The determination coefficient was only slightly weaker than for AvaSpec-256 measurements: 0.94 for UVB and 0.96 for UVA. Again, no systematic deflection was detected. The majority of ratios of measured daily doses to calculated daily doses stayed within the range 1 ± 0.2. The days with a larger divergence were days with very low daily doses (overcast sky), when the ratio values are more sensitive to absolute difference.

Later, the models have been also tested on measurement data from 2008–2013 to ensure its applicability for filling measurement caps. Altogether 949 full days with measurements were included into comparison. For UVB the determination coefficient r^2 was 0.94 (Figure 22 a). There was a small group of days (14 out of 949) that showed noticeably lower modelled values compared to actual measurements. Most of them were from April and May with almost clear sky. The most probable reason for underestimation of daily doses is in estimation of ozone influence. The model could have some problems in certain conditions separating spring with very high ozone values from fall with very low ozone values as all the other input parameters are similar for those seasons.

Another aspect with ozone values could be high variation in daily bases. Second reason for this deflection could be the enhancement of radiation by clouds (Sabburg and Parisi, 2006; Sabburg and Calbo, 2009). For UVA, the r^2 was 0.97 and no such abnormality was found (Figure 22 b), but there was some underestimation of daily doses, especially in case of high radiation levels. That was also shown on the data from 2007 (Figure 21).
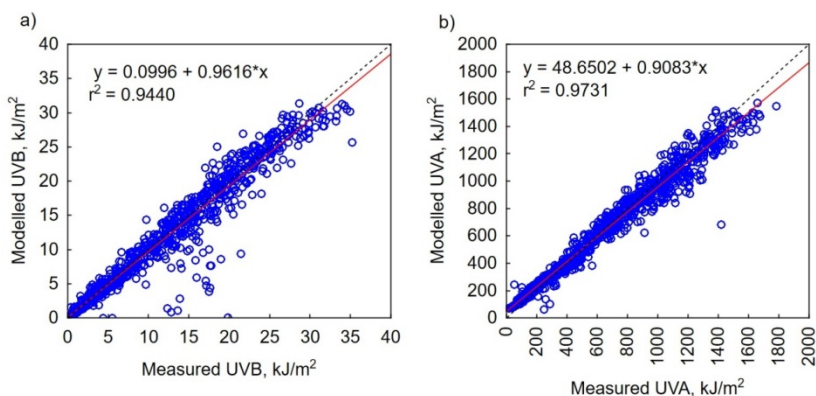

Figure 22. Scatterplot of measured and modelled a) UVB and b) UVA daily doses from 2008–2013. 949 days included.

3.5.3. Yearly doses of UV radiation since 1955

With the constructed models the daily UVB and UVA doses were calculated for 1955–2003. The period was extended with measurements combined with calculations (to fill gaps) until 2007. The yearly doses are in Figure 23.
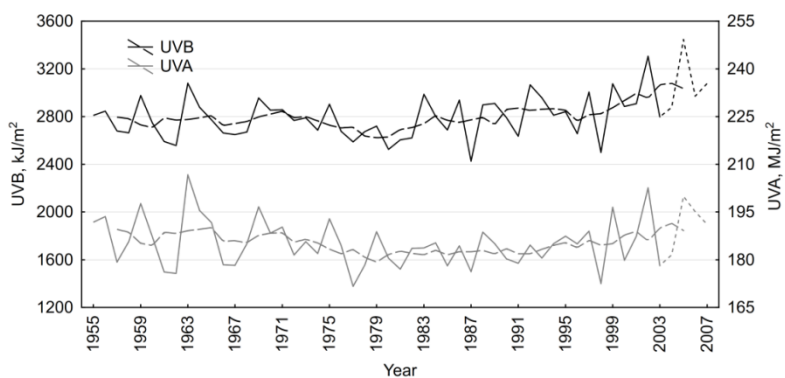

Figure 23. Yearly doses of UVB and UVA radiation with a 5-year moving average (dashed smoother line) from 1955 to 2007 at Tõravere. Reconstructed values until 2003 (solid line) and 2004–2007 measurements in combination with calculated values (dotted line).

The 5-year moving average shows higher levels of UVA and UVB radiation until the beginning of the 1970s. After that radiation levels declined. Minimum yearly doses were reached in 1979. While UVA stayed fairly constant on a lower level until the middle of the 1990s, UVB started to increase since the 1980s, exceeding its values in the 1960s by the beginning of the 2000s. For comparison with other authors, a linear trend from 1979–2003 was calculated and 4.1% increase per decade in UVB and about 1% increase per decade in UVA was found. Similar trends since the 1980s have been described by many other authors. Bilbao *et al.* (2011) found an upward trend of 3.5% per decade for the erythemal UV radiation in Spain in summer. Outer *et al.* (2010) described an increase in the erythemal UV radiation level since the 1980s in various sites in Europe. The radiation level by the end of 2010s was found to be 4–8% higher than before the 1980s. An increase of the UVB radiation was also detected by Krzyścin (2003) as a linear trend of 2.5% per decade for the snowless part of the year in 1988–2000 at Belsk, Poland; Lindfors and Vuilleumier (2005) noted a linear upward trend of erythemal UV yearly doses in 1979–1999 at Davos, Switzerland. It must be noted that no long-term conclusions can be made based on reported trends – these are relevant only in selected timeframe. For understanding changes in the climate much longer time series of measurements are needed. Considering another meteorological para-meter, precipitations, data for Estonia are available already from 1866 and a 25–30 year periodicity was found (Järvet and Jaagus, 1996; Nõges *et al.*, 2012).

In our later work the yearly doses period was even more extended with measurements combined with calculations from 2008 to 2013 and with solely calculations from 2014 to 2015. The results are presented in Figure 24. It shows peak values in 2011 – a year with high global solar radiation, caused by lower than average cloudiness, and low column ozone level. For the past few years the amount of UV radiation, received on ground during a year, has gone down.
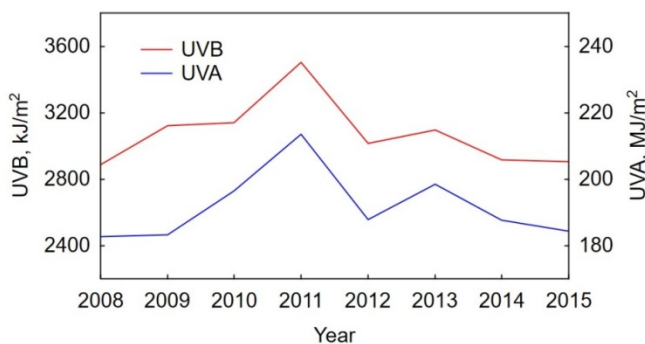

Figure 24. Yearly doses of UVB (red line) and UVA (blue) from 2008 to 2015 at Tõra-vere. Period from 2008–2013 is combination of measured and modelled daily doses, 2014–2015 only modelled values.

The results of the present reconstruction were also compared with the results of reconstructed erythemal UV doses at Tõravere (Eerme *et al.*, 2002b; 2006) and with the results of broadband radiation studies for the same site (Eerme *et al.*, 2010; Eerme and Aun, 2012). Changes in yearly doses acted similarly in the two reconstructions. For the reconstructed erythemal radiation for Tõravere the upward trend since 1979 was 3.6% per decade. The determination coefficient between UVB and erythemal radiation from the two reconstructions was 0.8. When the two reconstructed yearly dose values are normalized from 0 to 1, the difference between the two reconstructions is between –0.15 and 0.2 with three exceptions: distinctive mismatches occur in the years 1983, 1992, and 1993 (Figure 25), where the later reconstruction shows larger values. The reason for the divergence of the two reconstructions seems to come from the different impact of ozone on UVB and erythemal radiation and its consideration in models. Yearly doses of UVB have a much stronger correlation with ozone (–0.57) than yearly doses of erythemal radiation. The period from the beginning of the 1980s until the middle of the 1990s manifests a decline in average ozone values with local minimums in 1983, 1992, and 1993, mentioned above as the years of a mismatch between the two reconstructions. Those minimums follow two large volcanic eruptions: those of El Chichón (1982) and Mount Pinatubo (1991). Aerosols transported into the atmosphere from a volcanic event change the chemistry of the atmosphere and have a destructive effect on ozone (Glasow *et al.*, 2009). Also the reconstruction of erythemal doses uses turbidity as a separate factor to account for changes in aerosol. The reconstruction for erythemal radiation is more strongly correlated with global solar radiation (0.89, for UVB 0.67).
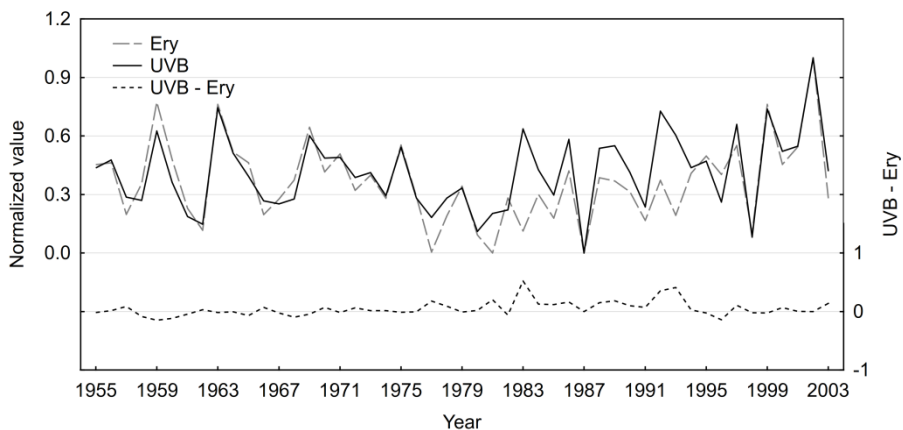

Figure 25. Normalized reconstructed yearly doses of UVB and erythemal (Ery) UV from 1955 to 2003 at Tõravere.

Changes in global solar radiation and column ozone also support the results of the reconstruction. Especially high yearly doses of UV are presented when yearly total solar radiation is high and at the same time average ozone level is low (important in UVB band), like in year 2011 (Figure 26). Correlation between UVA and global solar radiation is very high ($r^2 = 0.98$) as expected. A more moderate correlation is found with UVB (0.67). At the same time yearly mean O_3 has a statistically significant negative correlation (–0.57) with UVB doses, playing a major role in shaping the final dose received on the ground. Global solar radiation varies mainly due to cloudiness. These variations for Tõravere are described in this thesis in Section 3.2.
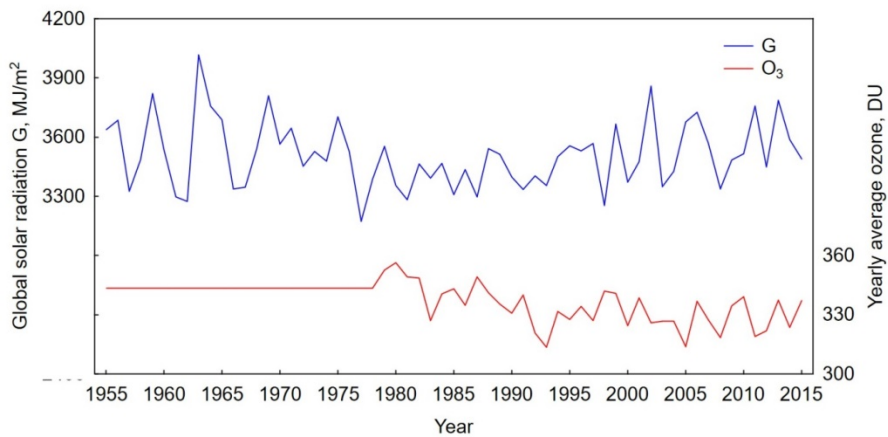

Figure 26. Changes in yearly global solar radiation and yearly average global ozone from 1955–2015.

4. CONCLUSIONS

Due to various effects of UV radiation on ecosystems and materials there is a necessity to assess quantitatively UV daily exposures and describe their long-term variations. The available irradiance levels and doses are site specific, because maximum available solar radiation dependence on latitude and the weather conditions are influenced by geographical location.

The measurements of UV spectral radiation started at Tõravere in 2004 with array minispectrometer AvaSpec-256. In 2009 it was replaced by Bentham DMc-150 instrument. Twelve years of spectral UV radiation measurements (2004–2015) in combination with data collected at the nearby Tartu-Tõravere meteorological station have given a large dataset for analysing the daily, seasonal and long-term changes of UV irradiances and doses. Also it has given an opportunity to study the effect of different atmospheric conditions like cloudiness and aerosol on UV radiation.

Summary of the main results of the thesis:

1. Main features of the UV spectra at Tõravere were found. Detectable spectra start from wavelength 295 to 310 nm depending mainly on the SZA. With changing SZA the ratio UVA/UVB varies and can change by more than ten times from sunrise/sunset to noon. During summer close to 90% of radiation at 300 nm is received during 6 noon hours, from 330 nm, towards longer wavelengths, contribution of the 6 noon hours stays on a almost constant level of 60%. The daily dose of UVB can reach over 30 kJ/m^2 during summer and UVA over 1500 kJ/m^2, around winter solstice the values are only 0.10 to 0.20 kJ/m^2 and 30 to 70 kJ/m^2, respectively.

    The work gives a quantitative description of daily and annual change in UV radiation levels and spectral composition in Estonia. Knowing the maximum possible irradiances and doses for certain periods gives an opportunity in the future to estimate energy available for different processes. Also the estimation of the modification of ground-level UV radiation in all-weather conditions is possible.

2. Analysis of the entire dataset of UV spectra as well as single case studies gave a reliable quantitative estimation of clouds and aerosol effects on spectral UV radiation and available radiation levels in cloudy conditions. UV doses in overcast days are about 1/3 from the clear weather ones and wavelength dependency was shown (CMF = 0.38 at 332 nm and 0.36 at 386 nm). The average CMF of low level clouds in UVB region is 0.35 for *Ns* and 0.45 for *St* and for medium level clouds 0.61 for *As* and 0.66 for *Ac*. Still the separation of cloud types by a single UV spectrum is not possible – single case studies showed a large variation of the CMF in frames of a certain cloud type.

    Although the effect of clouds and wavelength dependency of it is known from earlier studies, our work helps to improve the quantification of the effect of different cloud types. Understanding and quantifying the reduction/

enhancement of UV irradiance due to changing climatic factors helps to assess the real energy available for different biological and chemical processes like vitamin D synthesis.

3. Analysis of cloud time series from 1958 to 2011 enabled a quantification of seasonal cycle for average sum of medium and low level clouds in 10-day intervals (max. value of 8 in November and min. of 5, in the end of April). A specific feature in long-term changes in cloudiness from 1992–1996 (increase of cloudiness due to volcanic eruption) was detected. The number of days with clear sky at ± 2 h from noon has been lower since the end of the 1980s and especially since 2008.

4. An easy and accessible modelling method for UV daily doses is proposed, using ARESLab and libRadtran software and daily global solar radiation, ozone, noon SZA and calculated clear sky daily doses as input. Although there have been several models developed and published many of them are specific to erythemal UV. We were interested in a flexible method that easily enables greating new models and that the models performance would be as close to maximum as possible.

5. Appropriate models for UVB and UVA daily dose calculations were created on the basis of Tõravere site data, r^2 close to 0.95 appeared for both studied wavelength ranges.

6. Reconstruction of UVB and UVA daily doses back to 1955 for Tõravere site showed the decline in UV doses since the beginning of the 1970s up to the beginning of the 1980s. The UVB values increased since the 1980s until recent years, the UVA doses stayed on a lower level until the 1990s. The increase of UV annual doses stopped at 2011 and have decreased since then.

   The results are applicable for the most area of Estonia and partly for neighboring countries.

In the future, as the models have shown reliable results compared to measurements, they will be continuously in work for supporting the measurements and helping to keep the dataset uniform. Although models described in the thesis are site specific, new models, using the same method can fairly easily be developed for different location and different wavelength band or for action spectra applied radiation. As a next step the method will be applied for building a model for vitamin D synthesis studies.

Another plan is to analyse the data from measurements of diffuse UV radiation that have been carried out since summer 2016 at Tartu Observatory. A lot of new information could be received.

REFERENCES

Amiridis, V., Giannakaki, E., Balis, D. S., Gerasopoulos, E., Pytharoulis, I., Zanis, P., Kazadzis, S., Melas, D., Zerefos, C., 2010. Smoke injection heights from agricultural burning in Eastern Europe as seen by CALIPSO. *Atmos. Chem. Phys.* 10, 11567–11576. doi:10.5194acp-10-11567–2010

Ansko, I., Eerme, K., Lätt, S., Noorma, M., Veismann, U., 2008. Study of suitability of AvaSpec array spectrometer for solar UV field measurements. *Atmos. Chem. Phys.* 8, 3247–3253.

Arola, A., Lindfors, A., Natunen, A., Lehtinen, K. E. J., 2007. A case study on biomass burning aerosols: effects on aerosol optical properties and surface radiation levels. *Atmos. Chem. Phys.* 7, 4257–4266.

ASTM, 2000. Standard Solar Constant and Zero Air Mass Solar Spectral Irradiance Tables. American Society for Testing and Materials, West Conshohocken, PA.

Aun, M., Eerme, K., Ansko, I., Veismann, U., Lätt, S., 2011. Modification of Spectral Ultraviolet Doses by Different Types of Overcast Cloudiness and Atmospheric Aerosol. *Photochem. Photobiol.* 87, 461–469.

Baczynska, K. A., Price, L. L. A., Higlett, M. P., O'Hagan, J. B., 2016. Estimating Sun Exposure of Children in Day Care Nurseries in South Oxfordshire, UK. *Photochem. Photobiol.* 92, 193–200. doi:10.1111/php.12536

Barnaba, F., Angelini, F., Curci, G., Gobbi, G. P., 2011. An important fingerprint of wildfires on the European aerosol load. *Atmos. Chem. Phys.* 11, 10487–10501. doi:10.5194/acp-11-10487-2011

Bilbao, J., Roman, R., de Miguel, A., Mateos, D., 2011. Long-term solar erythemal UV irradiance data reconstruction in Spain using a semiempirical method. *J. Geophys. Res. Atmospheres* 116, D22211, 15 p.

Björn, L. O., 2007. Stratospheric ozone, ultraviolet radiation, and cryptogams. *Biol. Conserv.* 135, 326–333. doi:http://dx.doi.org/10.1016/j.biocon.2006.10.006

Bodekær, M., Harrison, G. I., Philipsen, P., Petersen, B., Triguero-Mas, M., Schmalwieser, A. W., Rogowski-Tylman, M., Dadvand, P., Lesiak, A., Narbutt, J., Eriksen, P., Heydenreich, J., Nieuwenhuijsen, M., Thieden, E., Young, A. R., Wulf, H. C., 2015. Personal UVR exposure of farming families in four European countries. *J. Photochem. Photobiol. B* 153, 267–275. doi:http://dx.doi.org/10.1016/j.jphotobiol.2015.10.002

Brown, S. W., Johnson, B. C., Feinholz, M. E., Yarbrough, M. A., Flora, S. J., Lykke, K. R., Clark, D. K., 2003. Stray-light correction algorithm for spectrographs. *Metrologia* 40, S81.

Burrows, W. R., 1997. CART Regression Models for Predicting UV Radiation at the Ground in the Presence of Cloud and Other Environmental Factors. *J. Appl. Meteorol.* 36, 531–544.

Calbó, J., Pagès, D., González, J. A., 2005. Empirical studies of cloud effects on UV radiation: A review. *Rev. Geophys.* 43, RG2002, 28 p. doi:10.1029/2004RG000155

Caldwell, M. M., Bornman, J. F., Ballare, C. L., Flint, S. D., Kulandaivelu, G., 2007. Terrestrial ecosystems, increased solar ultraviolet radiation, and interactions with other climate change factors. *Photochem. Photobiol. Sci.* 6, 252–266. doi:10.1039/B700019G

CIE, 1987. CIE International Lighting Vocabulary: IEC International Electrotechnical Vocabulary, CIE Publication. CIE.

Cutforth, H. W., Judiesch, D., 2007. Long-term changes to incoming solar energy on the Canadian Prairie. *Agric. For. Meteorol*. 145, 167–175.

De Gruijl, F. R., Rebel, H., 2008. Early Events in UV Carcinogenesis – DNA Damage, Target Cells and Mutant p53 Foci†. *Photochem. Photobiol.* 84, 382–387. doi:10.1111/j.1751-1097.2007.00275.x

Eerme, K., 2004. Changes in spring–summer cirrus cloud amount over Estonia, 1958–2003. *Int. J. Climatol*. 24, 1543–1549. doi:10.1002/joc.1055

Eerme, K., 2012. Interannual and Intraseasonal Variations of the Available Solar Radiation, Babatunde, in: E.B. (Ed.), Solar Radiation. InTech, 33–52.

Eerme, K., Aun, M., 2012. A Review of the Variations of Optical Remote Sensing Conditions over Estonia in 1958–2011. *Int. J. Remote Sens. Appl*. 2, 12.

Eerme, K., Aun, M., Veismann, U., 2015. Instrumentation and Measurement of Ground-Level Ultraviolet Irradiance and Spectral Composition in Estonia, in: Solar Radiation Applications. InTech, 119–139.

Eerme, K., Kallis, A., Veismann, U., Ansko, I., 2010. Long-term variations of available solar radiation on seasonal timescales in 1955–2006 at Tartu-Tõravere Meteorological Station, Estonia. *Theor. Appl. Climatol.* 101, 371–379.

Eerme, K., Veismann, U., Ansko, I., Lätt, S., 2006. Year-to-year variations of the vitamin D synthesis related UV-B radiation in Estonia in autumn and spring, in: Proceedings of the SPIE, 7 p.

Eerme, K., Veismann, U., Koppel, R., 2000. Ultraviolet irradiance in meteorologically contrasting summers of 1998 and 1999 in Estonia. *Proc. Est. Acad. Sci. Phys. Math.* 49, 250–264.

Eerme, K., Veismann, U., Koppel, R., 2002a. Estonian total ozone climatology. *Ann. Geophys.* 20, 247–255. doi:10.5194/angeo-20-247-2002

Eerme, K., Veismann, U., Koppel, R., 2002b. Variations of erythemal ultraviolet irradiance and dose at Tartu/Tõravere, Estonia. *Clim. Res.* 22, 245–253.

Eerme, K., Veismann, U., Koppel, R., Pehk, M., 1998. First four years of atmospheric total ozone measurements in Estonia. *Proc. Est. Acad. Sci. Biol. Ecol.* 188–202.

Eerme, K., Veismann, U., Lätt, S., 2006. Proxy-based reconstruction of erythemal UV doses over Estonia for 1955–2004. *Ann. Geophys.* 24, 1767–1782.

Feister, U., Cabrol, N., Häder, D., 2015. UV Irradiance Enhancements by Scattering of Solar Radiation from Clouds. *Atmosphere* 6, 1211–1228. doi:10.3390/atmos6081211

Feister, U., Junk, J., Woldt, M., Bais, A., Helbig, A., Janouch, M., Josefsson, W., Kazantzidis, A., Lindfors, A., Outer, P.N. den, Slaper, H., 2008. Long-term solar UV radiation reconstructed by ANN modelling with emphasis on spatial characteristics of input data. *Atmos. Chem. Phys*. 8, 3107–3118.

Foukal, P., 1990. *Solar astrophysics*. A Wiley-Interscience Publication, 496 p.

Foyo-Moreno, I., Alados, I., Olmo, F. J., Alados-Arboledas, L., 2003. The influence of cloudiness on UV global irradiance (295–385 nm). *Agric. For. Meteorol.* 120, 101–111.

Frederick, J. E., Steele, H. D., 1995. The Transmission of Sunlight through Cloudy Skies: An Analysis Based on Standard Meteorological Information. *J. Appl. Meteorol*. 34, 2755–2761.

Friedman, J. H., 1991. Multivariate Adaptive Regression Splines. *Ann. Stat*. 19, 1–67.

Fröhlich, C., Brusa, R. W., 1981. Solar Radiation and its Variation in Time, in: Domingo, V. (Ed.), Physics of Solar Variations: Proceedings of the 14th ESLAB Symposium Held in Scheveningen, The Netherlands, 16–19 September, 1980. Springer Netherlands, Dordrecht, 209–215.

Glasow, R. von, Bobrowski, N., Kern, C., 2009. The effects of volcanic eruptions on atmospheric chemistry. *Chem. Geol.* 263, 131–142.

Haberreiter, M., Krivova, N. A., Schmutz, W., Wenzler, T., 2005. Reconstruction of the solar UV irradiance back to 1974. *Adv. Space Res*. 35, 365–369.

Hader, D.-P., Kumar, H. D., Smith, R. C., Worrest, R. C., 2007. Effects of solar UV radiation on aquatic ecosystems and interactions with climate change. *Photochem. Photobiol. Sci* 6, 267–285. doi:10.1039/B700020K

Holben B. N., Eck, T. F., Slutsker, I., Tanre, D., Buis, J.P., Setzer, A., Vermote, E., Reagan, J.A., Kaufman, Y., Nakajima, T., Lavenu, F., Jankowiak, I., Smirnov, A., 1998: AERONET – A federated instrument network and data archive for aerosol characterization, *Rem. Sens. Environ.*, 66, 1–16.

Jackson, S. P., Bartek, J., 2009. The DNA-damage response in human biology and disease. *Nature* 461, 1071–1078. doi:10.1038/nature08467

Järvet, A., Jaagus, J., 1996. The impact of climate change on hydrological regime and water resources in Estonia, in: Punning, J. (Ed.), Estonia in the System of Global Climate Change. Institute of Ecology, Tallinn, 84–103.

Jekabsons, G., 2011. ARESLab, Adaptive Regression Splines toolbox for Matlab/ Octave.

Junk, J., Feister, U., Helbig, A., Görgen, K., Rozanov, E., Krzyscin, J. W., Hoffmann, L., 2012. The benefit of modeled ozone data for the reconstruction of a 99-year UV radiation time series. *J. Geophys. Res. Atmospheres* 117, D16102, 10 p.

Kakani, V. G., Reddy, K. R., Zhao, D., Sailaja, K., 2003. Field crop responses to ultraviolet-B radiation: a review. *Agric. For. Meteorol*. 120, 191–218.

Kallis, A., Russak, V., Ohvril, H., 2005. 100 years of solar radiation measurements in Estonia, in: WCRP Informal Report. Presented at the The Eighth Session of the Baseline Surface Radiation Network (BSRN) Workshop and Scientific Review, Exeter, UK, C1–C4.

Kambezidis, H. D., Kaskaoutis, D. G., Kharol, S. K., Moorthy, K. K., Satheesh, S. K., Kalapureddy, M. C. R., Badarinath, K. V. S., Sharma, A. R., Wild, M., 2012. Multi-decadal variation of the net downward shortwave radiation over south Asia: The solar dimming effect. *Atmos. Environ.* 50, 360–372.

Kannel, M., Ohvril, H., Okulov, O., 2012: A shortcut from broadband to spectral aerosol optical depth. *Proc. Estonian Acad. Sc*., 61, 4, 266–278, doi: 10.3176/ proc.2012.4.02.

Kannel, M., Ohvril, H., Okulov, O., Kattai, K., Neiman, L., 2014. Spectral aerosol optical depth prediction by some broadband models. Validation with AERONET observations. *Proc. Estonian Acad. Sc.* 63, 4, 404–416, doi: 10.3176/proc.2014.4.06

Kataria, S., Jajoo, A., Guruprasad, K. N., 2014. Impact of increasing Ultraviolet-B (UV-B) radiation on photosynthetic processes. *J. Photochem. Photobiol. B* 137, 55–66. doi:http://dx.doi.org/10.1016/j.jphotobiol.2014.02.004

Kaurola, J., Taalas, P., Koskela, T., Borkowski, J., Josefsson, W., 2000. Long-term variations of UV-B doses at three stations in northern Europe. *J. Geophys. Res. Atmospheres* 105, 20813–20820.

Keevallik, S., Russak, V., 2001. Changes in the amount of low clouds in Estonia (1955–1995). *Int. J. Climatol.* 21, 389–397. doi:10.1002/joc.618

Kostkowski, H. J., 1997. Reliable spectroradiometry. Spectroradiometry Consulting, La Plata, Md.

Krzyścin, J. W., 2003. Nonlinear (MARS) modeling of long-term variations of surface UV-B radiation as revealed from the analysis of Belsk, Poland data for the period 1976–2000. *Ann. Geophys.* 21, 1887–1896.

Krzyscin, J. W., Eerme, K., Janouch, M., 2004. Long-term variations of the UV-B radiation over Central Europe as derived from the reconstructed UV time series. *Ann. Geophys*. 22, 1473–1485.

Kylling, A., Albold, A., Seckmeyer, G., 1997. Transmittance of a cloud is wavelength-dependent in the UV-range: Physical interpretation. *Geophys. Res. Lett.* 24, 397–400. doi:10.1029/97GL00111

Lenoble, J., 1985. *Radiative transfer in scattering and absorbing atmospheres: standard computational procedures.* A. Deepak Pub., 300 p.

Lenoble, J., 1993. *Atmospheric radiative transfer, Studies in geophysical optics and remote sensing*. A. Deepak Pub., 532 p.

Lindfors, A., Kaurola, J., Arola, A., Koskela, T., Lakkala, K., Josefsson, W., Olseth, J. A., Johnsen, B., 2007. A method for reconstruction of past UV radiation based on radiative transfer modeling: Applied to four stations in northern Europe. *J. Geophys. Res. Atmospheres* 112, D23201, 15 p. doi:10.1029/2007JD008454

Lindfors, A., Vuilleumier, L., 2005. Erythemal UV at Davos (Switzerland), 1926–2003, estimated using total ozone, sunshine duration, and snow depth. *J. Geophys. Res. Atmospheres* 110, 1–15.

Lund Myhre, C., Toledano, C., Myhre, G., Stebel, K., Yttri, K. E., Aaltonen, V., Johnsrud, M., Frioud, M., Cachorro, V., de Frutos, A., Lihavainen, H., Campbell, J. R., Chaikovsky, A. P., Shiobara, M., Welton, E. J., Tørseth, K., 2007. Regional aerosol optical properties and radiative impact of the extreme smoke event in the European Arctic in spring 2006. *Atmos. Chem. Phys.* 7, 5899–5915. doi:10.5194/acp-7-5899-2007

Mayer, B., Kylling, A., 2005. Technical note: The libRadtran software package for radiative transfer calculations – description and examples of use. *Atmos. Chem. Phys.* 5, 1855–1877.

Mayer, B., Seckmeyer, G., Kylling, A., 1997. Systematic long-term comparison of spectral UV measurements and UVSPEC modeling results. *J Geophys. Res.* 102, 8755–8767.

McKenzie, R. L., Aucamp, P. J., Bais, A. F., Björn, L. O., Ilyas, M., 2007. Changes in biologically-active ultraviolet radiation reaching the Earth's surface. *Photochem. Photobiol. Sci.* 6, 218–231.

McKenzie, R. L., Liley, J. B., Björn, L. O., 2009. UV Radiation: Balancing Risks and Benefits†. *Photochem. Photobiol.* 85, 88–98. doi:10.1111/j.1751-1097.2008.00400.x

Medhaug, I., Olseth, J. A., Reuder, J., 2009. UV radiation and skin cancer in Norway. *J. Photochem. Photobiol. B* 96, 232–241.

Niemi, J. V., Tervahattu, H., Vehkamäki, H., Martikainen, J., Laakso, L., Kulmala, M., Aarnio, P., Koskentalo, T., Sillanpää, M., Makkonen, U., 2005. Characterization of aerosol particle episodes in Finland caused by wildfires in Eastern Europe. *Atmos. Chem. Phys*. 5, 2299–2310. doi:10.5194/acp-5-2299-2005

Nõges, P., Jaagus, J., Järvet, A., Nõges, T., Laas, A., 2012. Kliimamuutuse mõju veeökosüsteemidele ning põhjaveele Eestis ja sellest tulenevad veeseireprogrammi võimalikud arengusuunad. Estonian University of Life Sciences, Tartu, 249 p.

Ohvril, H., Teral, H., Neiman, L., Kannel, M., Uustare, M., Tee, M., Russak, V., Okulov, O., Jõeveer, A., Kallis, A., Ohvril, T., Terez, E. I., Terez, G.A., Gushchin, G. K., Abakumova, G. M., Gorbarenko, E. V., Tsvetkov, A. V., Laulainen, N., 2009.

Global dimming and brightening versus atmospheric column transparency, Europe, 1906–2007. *J. Geophys. Res. Atmospheres* 114, D00D12, 17 p. doi:10.1029/2008JD010644

Olds, W. J., 2010. Elucidating the links between UV radiation and vitamin D synthesis: using an in vitro model. Queensland University of Technology.

Orlova, T., Moan, J., Lagunova, Z., Aksnes, L., Terenetskaya, I., Juzeniene, A., 2013. Increase in serum 25-hydroxyvitamin-D3 in humans after sunbed exposures compared to previtamin {D3} synthesis in vitro. *J. Photochem. Photobiol.* B 122, 32–36. doi:http://dx.doi.org/10.1016/j.jphotobiol.2013.03.006

Outer, P. N. den, Slaper, H., Kaurola, J., Lindfors, A., Kazantzidis, A., Bais, A. F., Feister, U., Junk, J., Janouch, M., Josefsson, W., 2010. Reconstructing of erythemal ultraviolet radiation levels in Europe for the past 4 decades. *J. Geophys. Res. Atmospheres* 115, D10102, 17 p.

Outer, P. N. den, Slaper, H., Tax, R.B., 2005. UV radiation in the Netherlands: Assessing long-term variability and trends in relation to ozone and clouds. *J. Geophys. Res. Atmospheres* 110, D02203.

Parisi, A., Kimlin, M., 1997. Ozone and ultraviolet radiation. *Australas. Sci.* 18 (1), 44–46.

Reuder, J., Schwander, H., 1999. Aerosol effects on UV radiation in nonurban regions. *J. Geophys. Res. Atmospheres* 104, 4065–4077. doi:10.1029/1998JD200072

Rieder, H. E., Holawe, F., Simic, S., Blumthaler, M., Krzyŝcin, J. W., Wagner, J. E., Schmalwieser, A.W., Weihs, P., 2008. Reconstruction of erythemal UV-doses for two stations in Austria: A comparison between alpine and urban regions. *Atmos. Chem. Phys.* 8, 6309–6323.

Rieder, H. E., Staehelin, J., Weihs, P., Vuilleumier, L., Maeder, J. A., Holawe, F., Blumthaler, M., Lindfors, A., Peter, T., Simic, S., Spichtinger, P., Wagner, J. E., Walker, D., Ribatet, M., 2010. Relationship between high daily erythemal UV doses, total ozone, surface albedo and cloudiness: An analysis of 30 years of data from Switzerland and Austria. *Atmos. Res*. 98, 9–20.

Rösemann, R., Meijer, H. P., van der Voort, J., 2011. *A Guide to Solar Radiation Measurement: From Sensor to Application*. Kipp & Zonen, 218 p.

Russak, V., 1990. Trends of solar radiation, cloudiness and atmospheric transparency during recent decades in Estonia. *Tellus B* 42, 206–210.

Russak, V., 1996. Atmospheric aerosol variability in Estonia calculated from solar radiation measurements. *Tellus A* 48, 786–791.

Russak, V., Kallis, A., 2003. *Eesti kiirguskliima teatmik (Handbook of Estonian solar radiation climate)*. Eesti Meteoroloogia ja Hüdroloogia Instituut, Tallinn (in Estonian).

Russak, V., Kallis, A., Joeveer, A., Ohvril, H., Teral, H., 2007. Changes in the spectral aerosol optical thickness in Estonia (1951–2004)/Aerosooli spektraalse optilise paksuse muutused Eestis aastatel 1951–2004. *Proc. Est. Acad. Sci. Biol.* 56, 69.

Sabburg, J., Calbo, J., 2009. Five years of cloud enhanced surface UV radiation measurements at two sites (in the Northern and Southern Hemispheres). *Atmos. Res*. 93, 902–912.

Sabburg, J. M., Parisi, A. V., 2006. Spectral Dependency of Cloud Enhanced UV Irradiance. *Atmos. Res*. 81, 206.

Schwander, H., Koepke, P., Kaifel, A., Seckmeyer, G., 2002. Modification of spectral UV irradiance by clouds. *J. Geophys. Res.* 107, 4296.

Schwander, H., Mayer, B., Ruggaber, A., Albold, A., Seckmeyer, G., Koepke, P., 1999. Method to Determine Snow Albedo Values in the Ultraviolet for Radiative Transfer Modeling. *Appl.Opt.* 38, 3869–3875.

Seinfeld, J. H., Pandis, S. N., 2006. *Atmospheric Chemistry and Physics: From Air Pollution to Climate Change*, 2nd Edition. Wiley, 1232 p. ISBN: 978-0-471-72018-8

Staiger, H., Outer, P. N. den, Bais, A. F., Feister, U., Johnsen, B., Vuilleumier, L., 2008. Hourly resolved cloud modification factors in the ultraviolet. *Atmos. Chem. Phys. Discuss.* 8, 181–214.

Stanhill, G., 2005. Global dimming: A new aspect of climate change. *Weather* 60, 11–14.

Stapleton, A. E., 1992. Ultraviolet Radiation and Plants: Burning Questions. *The Plant Cell*, 4, 1353–1358.

Stohl, A., Berg, T., Burkhart, J. F., Fjæraa, A. M., Forster, C., Herber, A., Hov, Ø., Lunder, C., McMillan, W. W., Oltmans, S., Shiobara, M., Simpson, D., Solberg, S., Stebel, K., Strøm, J., Tørseth, K., Treffeisen, R., Virkkunen, K., Yttri, K. E., 2007. Arctic smoke – record high air pollution levels in the European Arctic due to agricultural fires in Eastern Europe in spring 2006. *Atmos. Chem. Phys.* 7, 511–534.

Veismann, U., Eerme, K., Koppel, R., 2000. Solar erythemal ultraviolet radiation in Estonia in 1998. *Proc. Est. Acad. Sci. Phys. Math*. 49, 122–132.

WHO, 2002. Global Solar UV Index. A Practical Guide, 18 p.

Wild, M., Gilgen, H., Roesch, A., Ohmura, A., Long, C. N., Dutton, E. G., Forgan, B., Kallis, A., Russak, V., Tsvetkov, A., 2005. From Dimming to Brightening: Decadal Changes in Solar Radiation at Earth's Surface. *Science* 308, 847–850.

Witte, J. C., Douglass, A. R., da Silva, A., Torres, O., Levy, R., Duncan, B. N., 2011. NASA A-Train and Terra observations of the 2010 Russian wildfires. *Atmos. Chem. Phys.* 11, 9287–9301. doi:10.5194/acp-11-9287-2011

WMO, 1992. Scientific Assessment of Ozone Depletion: 1991 (No. 25).

WMO, 1995. Scientific Assessment of Ozone Depletion: 1994, Global ozone Research and Monitoring Project. (No. 37).

WMO, 2007. Scientific Assessment of Ozone Depletion: 2006, Global Ozone Research and Monitoring Project (No. 50).

Ylianttila, L., Visuri, R., Huurto, L., Jokela, K., 2005. Evaluation of a Single-mono-chromator Diode Array Spectroradiometer for Sunbed UV-radiation Measurements. *Photochem. Photobiol.* 81, 333–341. doi:10.1562/2004-06-02-RA-184.1

Zerefos, C., Eleftheratos, K., Meleti, C., Kazadzis, S., Romanou, A., Ichoku, C., Tselioudis, G., Bais, A., 2009. Solar dimming and brightening over Thessaloniki, Greece, and Beijing, China. *Tellus B* 61, 657–665.

Zong, Y., Brown, S. W., Johnson, B. C., Lykke, K. R., Ohno, Y., 2006. Simple spectral stray light correction method for array spectroradiometers. *Appl. Opt.* 45. doi:10.1364/AO.45.001111

SUMMARY IN ESTONIAN

Ultraviolettkiirguse sõltuvus kliimateguritest.
Eesti varasemate UV-kiirguse dooside arvutamine

Ultraviolettkiirguseks (UV-kiirgus) nimetatakse elektromagnetkiirgust laine-pikkuste vahemikus 10–400 nm. Pidades silmas Päikese kiirgusspektrit ja päiksekiirguse levi Maa atmosfääris, on erilise tähelepanu all maapinnani jõudev UV-kiirgus lainepikkuste vahemikus 280–400 nm, mis on jaotatud vastavalt kaheks osaks: 1) UVB (280–315 nm), 2) UVA (315–400 nm). Suure kvandienergia tõttu mõjustab UV-kiirgus nii eluslooudust kui looduslikke ja tehismaterjale. Ei ole lihtsat vastust küsimusele, kas UV-kiirgus on kasulik või kahjulik. See sõltub nii atmosfääriolude tõttu kujunenud UV-kiirguse spektrist kui kiirguse mõjumise ajast, seega siis UV-doosist ning organismi või materjali individuaalsest vastupanuvõimest kiirgusele. Suurtes doosides mõjub UV-kiirgus aga alati hävitavalt bioloogilistele kudedele ning looduslikele ja kunst-materjalidele. Seevastu väikeses koguses on UV-kiirgus inimorganismile häda-vajalik, aidates sünteesida D-vitamiini, vältida rahhiiti, tugevdada luustikku ja immuunsussüsteemi.

Mõistmaks, kuidas UV-kiirgus mõjustab meie keskkonnatingimusi, millised oleksid soovitused ja hoiatused, tuleb UV-kiirgust ja selle muutlikkust uurida. Eestis alustati regulaarseid UV-kiirguse lairiba-sensormõõtmisi Tartu-Tõravere meteojaamas 1998. aastal. Hoopis detailsem UV-kiirguse spektraalmonitooring sai võimalikuks alates 2004. aastast, mil Tartu Observatooriumis, Tõraveres, rakendati tööle rahvusvaheliselt firmalt Avantes ostetud minispetromeeter AvaSpec-256, mis 2009. aastal asendati briti firma Bentham Instruments Ltd spektromeetriga Bentham DMc-150. Kogu UV-kiirguse mõõtmisprotsess Tartu Observatooriumis on täielikul arvutijuhtimisel, mõõtmistsükkel kordub iga 15 minuti järel. Aastate jooksul on Tõreveres arhiveeritud ulatuslik UV-spektrite kogum, mida on täiendatud Tartu-Tõravere ilmajaama andmetega. Selle andme-baasi jätkuvale analüüsile ongi pühendatud käesolev doktoritöö, mida võiks ka nimetada UV-kiirguse füüsikaliseks klimatoloogiaks Tõraveres.

Vaatluse all olid nii üle lainepikkuste integreeritud UVB- ja UVA-kiirguse kiiritustihedused ja doosid kui ka valitud lainepikkustel registreeritud kiiritus-tihedused ning spektraalsed doosid.

Analüüsi tulemusena ilmnes, et suvel selge ilmaga ulatuvad maksimaalsed UVB päevased doosid Tõraveres üle 30 kJ/m^2 ning UVA doosid üle 1500 kJ/m^2. Südatalvel võivad need olla vastavalt kuni 300 korda ja 50 korda väiksemad. Suurimad kiiritustiheduse hetkväärtused esinevad suviste keskpäevade ümbru-ses, mil päikese kõrgus on Tõraveres maksimaalne. Vastavad UV-indeksi väär-tused ületavad juunis–juulis 7. Märgime, et ohtlikuks peetakse UV-indekseid alates väärtusest 6 ning esmased päikesekaitse meetmed tuleks Maailma Tervis-hoiu Organisatsiooni (WHO) soovitusel kasutusele võtta juba kui UV indeks on 3.

Kiirguse toime suhtes on oluline selle spektraalne koostis, mis muutub koos päikese kõrgusega. Suvel muutub suhe UVA/UVB suurusjärgust 500–600 hommikul suuruseni umbes 50 keskpäeval, mis tähendab, et suurem osa energeetiliselt aktiivsemast UVB kiirgusest saadakse just keskpäeva ümber. Enamasti ei õnnestu registreerida kiiritustiheduse usaldusväärseid väärtusi Tõraveres lühematel lainepikkustel kui 295 nm, kuid sõltuvalt tingimustest võib see piir olla isegi 310 nm juures.

Suur osa doktoritööst on pühendatud pilvede mõju uurimisele UV-kiirgusele, aluseks on võetud selge ilma UV-tase. Lauspilves taeva puhul moodustavad päevased doosid ligikaudu 1/3 selge ilma doosidest. Siit järeldub, et mõõduka UV-doosi võib saada ka pilves ilmaga. Täpsem analüüs näitas, et pilvede mõju UV-kiirgusele sõltub lainepikkusest – UVA ehk mahedama UV-kiirguse piir-konnas on enam mõjutatud pikemad lainepikkused ja maapinnani jõuab vähem kiirgust. Seda põhjustab erineva lainepikkusega kiirguse erinev hajumine. Eraldi on töös vaadeldud levinud pilvetüüpide, *St*, *Ns*, *As* ja *Ac*, pilvede mõju-faktorit ehk pilvise ilma UVB- ja UVA-kiirguse suhet selge ilma väärtusesse. Kuigi suure andmehulga keskmised pilvede mõjufaktorid erinesid alumiste (*St*, *Ns*) ja keskmiste (*As*, *Ac*) pilvede puhul, oli üksikult vaadates varieeruvus suur ja seetõttu ei ole võimalik pilveliike eristada pilve mõjufaktori järgi. Isegi paksud pilvekihid ei ole nii ühtlased, kui silmale tunduvad.

UV-kiirguse ajaliste muutuste paremaks tõlgendamiseks analüüsisime ka pilvisuse enda muutlikkust nii kuude kui aastate lõikes. Suurim on taevasfääri kaetus keskmiste ning alumiste pilvedega novembris ning detsembris, mil kuukeskmine kogu taevasfääri kaetus ületab 8 palli. Kõige väiksem on kuu-keskmine pilvisus keskmiste ning alumiste pilvede korral kevadkuudel (aprill, mai, juuni), ligikaudu 5 palli. Päevade arv aastas, kus keskpäeva ümber (± 2 tundi keskpäevast) on pilvevaba ja seega saabuvad kiirgushulgad suuremad, on vähenenud alates 1980ndate lõpust. Kuude lõikes esineb pilvevaba keskpäeva enim märtsis, aprillis ja mais. Suvel päikselise ilmaga (kõrgrõhkkkond) ilmuvad keskpäeva eel taevasse õhukesed konvektiivsed, nn ilusa ilma pilved (*Cu*), mille nii horisontaal- eriti aga vertikaalmõõtmed on keskpäevaks kasvanud suuren-dades taevasfääri kaetust ja vähendades maapinnani jõudvat UV-kiirgust.

Lisaks olemasolevate, Tõraveres mõõdetud UV-kiirguse andmete analüüsile, koostati doktoritöö raames ka mudelid UV-kiirgustaseme arvutamiseks. Selline arvutusmetoodika teiste keskkonnaparameetrite alusel annab võimaluse piken-dada UV-kiirguse aegridasid minevikku, kui UV-mõõtmisi veel ei toimunud, aga ka täita tehnilistel põhjustel tekkinud tühikuid olemasolevates UV-aeg-ridades. Et UV-kiirgusdoosid on tihedas korrelatsioonis päikese summaarse kiirguse ja osoonihulgaga, ongi need tähtsaimad UV-kiirguse rekonstrueerimise lähtesuurused. Päikese seniitnurk, pilvisuse hulk ja aerosoolid on "peidus" summaarses kiirguses, kuid neid võib üritada ka eraldi arvestada, samuti nagu ka lumikatet.

Käesolevas doktoritöös on UV-päevadooside modelleerimiseks kasutatud kahte tarkvarapaketti, vastavalt ARESLab ja libRadtran. Neist esimene kujutab endast adaptiivset (iseõppivat) regressioonanalüüsi, mis korrigeerib ennast nn

treeningtsüklite käigus. Teine pakett on loodud spetsiaalselt atmosfääri kiirgus-voogude arvutamiseks. Mudelite sisendsuurustena on väitekirjas kasutatud summaarset päikesekiirgust, atmosfääri taandatud osoonikihi paksust, kesk-päevast päikese seniitkaugust ning selge taeva päevaseid UV doose. Mudelite abil õnnestus taastada UV-päevadoosid perioodiks 1955–2003, see on ajaks, mis eelnes spektraalsetele mõõtmistele, aga mille jaoks on arhiveeritud Tõra-veres mõõdetud päikese summaarse kiirguse päevasummad. Kombineerides mõõdetud ja modelleeritud suurusi on koostatud Tõravere UV-dooside aegrida kuni aastani 2015. Ilmnes, et UV-kiirguse aastadoosid olid kõrged kuni 1970ndateni, seejärel UV-doosid vähenesid kuni 1980ndate alguseni. Alates 1980ndatest algas UVB ning 1990ndatest UVA dooside tõus ning 2000ndatetest alates on doosid suuremad, kui enne 1970ndaid. Maksimaalne aastane doos oli 2011. aastal, nii UVB kui UVA puhul. Saadud tulemusi võrreldi muutustega mõõdetud summaarses päikesekiirguse aastadoosides ning aasta keskmistes osooni hulkades. Muutused nii UVB- kui UVA-kiirguse aastadoosides on sel-gelt seotud muutustega summaarses kiirguses, mis omakorda on seotud eelkõige muutustega pilvisuses. Lisaks mängib olulist rolli UVB-kiirguse kogunemisel osoon ja maksimaalsed tasemed, nagu 2011. aastal, on saadud just suure summaarse päikesekiirguse ja madala osoonitaseme tõttu.

Edaspidi on UV päevadooside mudelid kasutuses UV-mõõtmistel parata-matute tehniliste rikete tõttu tekkivate tühimike täitmiseks ning aegridade katkematuse kindlustamiseks. Mudelid võimaldavad UV-dooside tasemetele hinnanguid anda isegi juhul, kui rahalistel põhjustel UV-spektrite mõõtmised Tõraveres peaksid katkema. Samuti on mudeli tegemisel loodud ja ka kirjel-datud meetod, mille abil on võimalik koostada uued mudelid erinevate laine-pikkuste vahemike või mõjuspektrite rakendamise korral. Ühtlasi on võimalik seda kasutada mudelite loomiseks mõnes teises geograafilises punktis.

.

ACKNOWLEDGEMENTS

PUBLICATIONS

CURRICULUM VITAE

Name: Margit Aun
Date of birth: May 14, 1985
E-mail: margit.aun@ut.ee

Education:

2009–...	University of Tartu, Environmental Technology, Doctoral Studies
2007–2009	University of Tartu, Environmental Technology, Master's Studies
2004–2007	University of Tartu, Environmental Technology, Bachelor's Studies
2002–2004	Nõo Science Gymnasium
2001–2002	Sir James Dunn Collegiate, Sault Ste Marie, Canada (as an exchange student)
2000–2001	Nõo Science Gymnasium

Special courses

2010	University of Tartu, Estonia, Learning and Teaching in Science Higher Education
2007	Tallinn University of Technology, Estonia, "Waves and coastal proccesses", summer school
2006	University of Utrecht, The Netherlands, "Physics of the Climate Systems", summer school

Teaching experience

2016	Environmental Physics I, Estonian University of Life Sciences
2015	Fundamentals of the Environmental Physics II, partial, University of Tartu
2014	Fundamentals of the Environmental Physics II, partial, University of Tartu
2012	Fundamentals of the Environmental Physics II, partial, University of Tartu
2010	Fundamentals of the Environmental Physics II, partial, University of Tartu

Career

2012–...	Tartu Observatory; Junior Research Fellow
2010.07.01–2010.11.30	Tartu Observatory; Specialist

Degree information

Margit Aun, Master's Degree, 2009, (sup) Kalju Eerme, Influence of cloudiness on ultraviolet radiation spectra measured in Tõravere, University of Tartu, Faculty of Science and Technology

Margit Aun, PhD Student, (sup) Hanno Ohvril, Kalju Eerme, UV spectral irradiance vs weather conditions, the past UV doses in Estonia, University of Tartu, Faculty of Science and Technology

Honours & Awards:
2010   Juhan Ross scholarship
2009   Juhan Ross scholarship

Participation in conferences and field projects:
2016, 13.–17. June, Nida, Lithuania. **1st Baltic Earth Conference**, Multiple drivers for Earth system changes in the Baltic Sea region. Oral presentation: "Changes in UV radiation in Estonia based on measurements and model calculations of UVA and UVB doses since 1955 at Tõravere"

2016, 12.–13. May, Tõravere, Estonia. **Nordic Ozone Group meeting**. Oral presentation: "UVB and UVA radiation since 2008 in Tõravere – measurements and calculations"

2015, 10.–14. August, Tartu, Estonia. **A Doctoral Students Conference "Challenges for Earth system science in the Baltic Sea region: From measurements to models"**. Oral presentation: "Reconstruction of UVB and UVA radiation at Tõravere, Estonia, for years 1955–2003"

2015, 7.–8. May, Copenhagen, Denmark. **Nordic Ozone Group meeting**. Oral presentation: "Recent work on UV radiation by atmospheric monitoring workgroup in Tartu Observatory, Estonia"

2009, 2.–3., April, Pärnu, Estonia. **Nordic Ozone Group meeting**. Oral presentation: "On the cloudiness induced variations in the spectral distribution of ground-level UV irradiance"

2006, Preila, Lithuania. ACCENT project. Investigation of Aerosol composition in Baltic Region, participation in *in situ* aerosol masurements

Publications:
Aun, M., Eerme, K., Aun, M., Ansko, I. (2016). Reconstruction of UVB and UVA radiation at Tõravere, Estonia, for the years 1955–2003. *Proceedings of the Estonian Academy of Sciences*, 65 (1), 50–57, 10.3176/proc.2016. 1.05.

Aun, M.; Eerme, K.; Aun, M.; Ansko, I. (2016). Changes in UV radiation in Estonia based on measurements and model calculations of UVA and UVB doses since 1955 at Tõravere. International Baltic Earth Secretariat Publication No. 9: 1st Baltic Earth Conference Multiple drivers for Earth system changes in the Baltic Sea region Nida, Curonian Spit, Lithuania 13– 17 June 2016. *International Baltic Earth Secretariat Publications*, 135–136.

Eerme, K., **Aun, M**., Veismann, U. (2015). instrumentation and measurement of ground-level ultraviolet irradiance and spectral composition in Estonia. In: Solar Radiation Applications (119–139). InTech.

Aun, M.; Eerme, K.; Aun, M.; Ansko, I. (2015). Reconstrucion of UVB and UVA radiation at Tõravere, Estonia, for years 1955–2003. International

Baltic Earth Secretariat Publication No. 5: A Doctoral Students Conference Challenges for Earth system science in the Baltic Sea region: From measurements to models University of Tartu and Vilsandi Island, Estonia, 10–14 August 2015. *International Baltic Earth Secretariat Publications*, 10–10.

Eerme, K.; **Aun, M**.; Veismann, U.; Ansko, I.; Vaštšenko, A.; Aruoja, I.; Virronen, K. (2014). Maapinnani jõudva päikesekiirguse muutlikkus ultra-violettpiirkonnas. Aan, Anne; Narusk, Kirke (Toim.). Kaugseire Eestis 2014 (156–165). Keskkonnaagentuur.

Eerme, K.; **Aun, M**. (2012). A Review of the Variations of Optical Remote Sensing Conditions over Estonia in 1958−2011. *International Journal of Remote Sensing Applications*, 2 (3), 12–19.

Aun, M.; Eerme, K.; Ansko, I.; Veismann, U.; Lätt, S. (2011). Modification of Spectral Ultraviolet Doses by Different Types of Overcast Cloudiness and Atmospheric Aerosol. *Photochemistry and Photobiology*, 87, 461–469.

ELULOOKIRJELDUS

Nimi: Margit Aun
Sünniaeg: 14. mai, 1985
E-mail: margit.aun@ut.ee

Haridus:
2009–... Tartu Ülikool, Keskkonnatehnoloogia, doktoriõpe
2007–2009 Tartu Ülikool, Keskkonnatehnoloogia, magistriõpe
2004–2007 Tartu Ülikool, Keskkonnatehnoloogia, bakalaureuseõpe
2002–2004 Nõo Reaalgümnaasium
2001–2002 Sir James Dunn Collegiate, Kanada (Rotary klubi vahetus-
          õpilane)
2000–2001 Nõo Reaalgümnaasium

Erikursused:
2010 Tartu Ülikool, Eesti, Õppimine ja õpetamine kõrgkoolis
2007 Tallinna Tehnikaülikool, Eesti, "Lained ja rannikuprotsessid",
     ingl. k, suvekool
2006 Utrechti Ülikool, Holland, "Kliimasüsteemide füüsika", ingl. k,
     suvekool

Õpetamine kõrgkoolis:
2016 Keskkonnafüüsika I, Eesti Maaülikool
2015 Keskkonafüüsika alused II, osa loengukursusest, Tartu Ülikool
2014 Keskkonafüüsika alused II, osa loengukursusest, Tartu Ülikool
2012 Keskkonafüüsika alused II, osa loengukursusest, Tartu Ülikool
2010 Keskkonafüüsika alused II, osa loengukursusest, Tartu Ülikool

Karjäär:
2012–... Tartu Observatoorium, nooremtadur
2010.07.01–2010.11.30 Tartu Observatoorium, spetsialist

Jätkuõpe:
Margit Aun, **magistrikraad**, 2009, (juh) Kalju Eerme, Tõraveres mõõdetud
   ultraviolettkiirguse spektri sõltuvus pilvisusest, Tartu Ülikool, Loodus- ja
   tehnoloogiateaduskond.
Margit Aun, **doktorant**, (juh) Hanno Ohvril; Kalju Eerme, UV-kiirguse
   spektraalkoostise sõltuvus ilmastikust, Eesti varasemad UV-doosid, Tartu
   Ülikool, Loodus- ja tehnoloogiateaduskond.

Auhinnad ja tunnustused:

2010   Juhan Rossi stipendium
2009   Juhan Ross stipendium

Osalemine konverentsidel ja välitöödel

2016, 13.–17. juuni, Nida, Leedu. **1st Baltic Earth Conference**, Multiple drivers for Earth system changes in the Baltic Sea region. Suuline ettekanne: "Changes in UV radiation in Estonia based on measurements and model calculations of UVA and UVB doses since 1955 at Tõravere"

2016, 12.–13. mai, Tõravere, Eesti. **Põhjamaade Osoonigrupi kokkusaamine**. Suuline ettekanne: "UVB and UVA radiation since 2008 in Tõravere – measurements and calculations"

2015, 10. –14. August, Tartu, Eesti. **Doktorantide konverents "Challenges for Earth system science in the Baltic Sea region: From measurements to models"**. Suuline ettekanne: "Reconstruction of UVB and UVA radiation at Tõravere, Estonia, for years 1955–2003"

2015, 7.–8. mai, Kopenhaagen, Taani. **Põhjamaade Osoonigrupi kokkusaamine**. Suuline ettekanne: "Recent work on UV radiation by atmospheric monitoring workgroup in Tartu Observatory, Estonia"

2009, 2.–3. aprill, Pärnu, Eesti. **Põhjamaade Osoonigrupi kokkusaamine**. Suuline ettekanne: „On the cloudiness induced variations in the spectral distribution of ground-level UV irradiance"

2006, Preila, Leedu. ACCENT projekt. Aerosooli koostise uurimine Läänemere regioonis, osalemine välitöödel aerosooli mõõtmisel

Publikatsioonid

Aun, M., Eerme, K., Aun, M., Ansko, I. (2016). Reconstruction of UVB and UVA radiation at Tõravere, Estonia, for the years 1955–2003. *Proceedings of the Estonian Academy of Sciences*, 65 (1), 50–57, 10.3176/proc.2016.1.05.

Aun, M.; Eerme, K.; Aun, M.; Ansko, I. (2016). Changes in UV radiation in Estonia based on measurements and model calculations of UVA and UVB doses since 1955 at Tõravere. International Baltic Earth Secretariat Publication No. 9: 1st Baltic Earth Conference Multiple drivers for Earth system changes in the Baltic Sea region Nida, Curonian Spit, Lithuania 13 - 17 June 2016. *International Baltic Earth Secretariat Publications*, 135–136.

Eerme, K., **Aun, M**., Veismann, U. (2015). instrumentation and measurement of ground-level ultraviolet irradiance and spectral composition in Estonia. In: Solar Radiation Applications (119–139). InTech.

Aun, M.; Eerme, K.; Aun, M.; Ansko, I. (2015). Reconstrucion of UVB and UVA radiation at Tõravere, Estonia, for years 1955-2003. International Baltic Earth Secretariat Publication No. 5: A Doctoral Students Conference Challenges for Earth system science in the Baltic Sea region: From measurements to models University of Tartu and Vilsandi Island, Estonia, 10–14 August 2015. *International Baltic Earth Secretariat Publications*, 10–10.

Eerme, K.; **Aun, M**.; Veismann, U.; Ansko, I.; Vaštšenko, A.; Aruoja, I.; Virronen, K. (2014). Maapinnani jõudva päikesekiirguse muutlikkus ultraviolettpiirkonnas. Aan, Anne; Narusk, Kirke (Toim.). Kaugseire Eestis 2014 (156–165). Keskkonnaagentuur

Eerme, K.; **Aun, M**. (2012). A Review of the Variations of Optical Remote Sensing Conditions over Estonia in 1958–2011. *International Journal of Remote Sensing Applications*, 2 (3), 12–19.

Aun, M.; Eerme, K.; Ansko, I.; Veismann, U.; Lätt, S. (2011). Modification of Spectral Ultraviolet Doses by Different Types of Overcast Cloudiness and Atmospheric Aerosol. *Photochemistry and Photobiology*, 87, 461–469.

DISSERTATIONES GEOPHYSICALES
UNIVERSITATIS TARTUENSIS

1. **Andres Kuusk.** The hot-spot effect in plant canopy reflectance. Tartu, 1991.
2. **Tiit Nilson.** Radiative transfer in non-homogeneous plant canopies. Tartu, 1991.
3. **Helgi Arst.** Atmosfääri ja mere kiirguskarakteristikud looduskeskkonna seisundi informaatoritena (vene keeles). Tartu, 1991.
4. **Juha Sarkkula.** Measuring and modelling water currents and quality as a part of decision making process for water pollution control. Tartu, 1992.
5. **Piia Post.** On the two radiatively effective cloud parameters. Tartu, 1993.
6. **Aadu Mirme.** Electric aerosol spectrometry. Tartu, 1994.
7. **Aare Luts.** Mathematical simulation of the evolutions of air ions. Tartu, 1995.
8. **Tiit Kutser.** Estimation of water quality in turbid inland and coastal waters by passive optical remote sensing. Tartu, 1997.
9. **Ülle Kikas.** Atmospheric aerosol in the Baltic region. Tartu, 1998.
10. **Tarmo Kõuts.** Processes of deep water renewal in the Baltic sea. Tartu, 1999.
11. **Anu Reinart.** Underwater light field characteristics in different types of Estonian and Finnish lakes. Tartu, 2000.
12. **Marko Kaasik.** Parameterisation of atmospheric boundary layer in the numerical model of air pollution transport. Tartu, 2000.
13. **Janek Laanearu.** Topographically constrained deep-water flows in channels. Tartu, 2001.
14. **Urmas Raudsepp.** Wind-driven circulation in the gulf of Riga. Tartu, 2001.
15. **Urmas Hõrrak.** Air ion mobility spectrum at a rural area. Tartu, 2001.
16. **Marko Vana.** Formation and evolution of atmospheric aerosol size spectrum by the occurrence of nucleation burst events in the atmospheric boundary layer; transport of the climatically active particulate air pollution. Tartu, 2002.
17. **Veljo Kimmel.** Analysis of methods of air quality assessment. Applications in Estonia. Tartu, 2002.
18. **Oleg Okulov.** Variability of atmospheric transparency and precipitable water in Estonia. Tartu, 2003.
19. **Aarne Männik.** Implementation and validation of the nonhydrostatic adiabatic core of the numerical weather prediction model hirlam. Tartu, 2003.
20. **Matti Mõttus.** Shortwave solar radiation field inside willow canopy. Tartu, 2004.
21. **Kalev Rannat.** Long weakly nonlinear waves in geophysical applications. Tartu, 2007.
22. **Rigel Kivi**. Observations of ozone, polar stratospheric cloud and water vapour profiles in the arctic. Tartu, 2007.

23. **Erko Jakobson.** Spatial and temporal variability of atmospheric column humidity. Tartu, 2009, 125 p.
24. **Sander Mirme.** Development of nanometer aerosol measurement technology. Tartu, 2011, 118 p.
25. **Hannes Keernik.** Estimating methods and variability of atmospheric humidity over the Baltic Region and the Arctic. Tartu, 2015, 105 p.
26. **Martin Kannel.** Development of Broadband Aerosol Optical Depth Models. Tartu, 2016, 168 p.
27. **Krista Alikas**. From research to applications: monitoring optically complex waters with MERIS/ENVISAT data. Tartu, 2016, 172 p.
28. **Velle Toll.** Direct radiative impacts of atmospheric aerosols on meteorological conditions over Europe. Tartu, 2016, 148 p.